host immune system to establish chronic infection, which often leads to serious liver diseases, such as cirrhosis and hepatocellular carcinoma. Even with a current standard treatment with pegylated interferon *plus* ribavirin, sustained viral clearance is obtained for only approximately 50% of patients infected with HCV genotype 1b (HCV-1b). Neither antibody-based prophylaxis nor an effective vaccine is currently available.

A better understanding of the interplay between viral and host factors that determine HCV clearance or persistence is needed for the design of effective passive immunotherapy and effective vaccines. A growing body of evidence from studies in humans and chimpanzees suggests that HCV-specific T-cell immunity plays an important role in the viral clearance [Bowen and Walker, 2005]. Also, several studies have indicated a role for humoral immunity in HCV infection [Bartosch et al., 2003; Logvinoff et al., 2004; Lavillette et al., 2005; Netski et al., 2005; Pestka et al., 2007; Dowd et al., 2009]. However, this aspect remains poorly characterized.

The E2 glycoprotein of HCV plays an important role in viral attachment and, therefore, becomes a major target of anti-HCV neutralizing antibodies. Identification of protective epitopes in E2 conserved among different HCV strains is a major challenge in vaccine design [Tarr et al., 2006; Helle et al., 2007; Gal-Tanamy et al., 2008; Keck et al., 2008]. The development of infectious retroviral pseudoparticles (HCVpp) bearing HCV envelope glycoproteins helps us study interactions between E2 epitopes and the virus receptor CD81 or neutralizing antibodies [Bartosch et al., 2003; Logvinoff et al., 2004; Lavillette et al., 2005; Pestka et al., 2007; Dowd et al., 2009]. More significantly, authentic HCV particles produced by the HCV cell culture system (HCVcc) are currently available for this purpose [Lindenbach et al., 2005; Wakita et al., 2005; Zhong et al., 2005; Fournier et al., 2007].

Recently, it was demonstrated using HCVcc that a mutation at position 534 from Asn to His (N534H) in the E2 glycoprotein of the HCV J6/JFH1 strain confers an advantage to the mutant viruses at the entry level probably through more efficient access to CD81 [Bungyoku et al., 2009]. The Asn-534 is located in the sixth of 11 *N*-linked glycosylation sites and the N534H mutation is predicted to remove this glycosylation. The present study has shown that the N534H mutation in the E2 glycoprotein of HCV J6/JFH1 markedly enhances the sensitivity of the virus to neutralization by specific neutralizing antibodies in sera of patients infected with HCV.

MATERIALS AND METHODS

Cells and Viruses

Huh-7.5 cells [Blight et al., 2002] and pFL-J6/JFH1 [Lindenbach et al., 2005] were kindly provided by Dr. C. M. Rice (Rockefeller University, New York, NY, USA). Huh-7.5 cells were cultured in Dulbecco's modified Eagle's medium (DMEM; Wako, Osaka, Japan) supplemented with 10% fetal bovine serum (Biowest, Nuaille, France), 0.1 mM non-essential amino acids (Invitrogen, Carlsbad, CA), penicillin (100 IU/ml), and streptomycin (100 μg/ml) (Invitrogen) at 37°C in a CO_2 incubator. Propagation of HCV J6/JFH1, its cell culture-adapted mutant P-47 and recombinant viruses possessing each of the adaptive mutations was described previously [Deng et al., 2008; Bungyoku et al., 2009].

Human Sera and Anti-HCV Neutralization Test

Sera were collected from 89 patients infected chronically with HCV-1b or HCV-2a, who were treated with pegylated interferon α-2b and ribavirin, as described previously [El-Shamy et al., 2007, 2008]. Sera were also collected from 11 patients with acute HCV-1b infection, either severe acute hepatitis or mild self-resolving hepatitis. The study protocol was approved by the Ethic Committees in Kobe University and Yamagata University and informed written consent provided by patients and volunteers. Sera collected from healthy volunteers who were negative for anti-HCV antibodies served as a control. The sera were inactivated at 56°C for 30 min before being used for the virus neutralization test.

An HCV neutralization test was performed as described previously [Sasayama et al., 2010]. In brief, serially diluted serum samples were mixed with the same amount of HCV solution containing 1×10^4 cell-infecting units. After incubation at 37°C for 1 hr, the mixtures were inoculated to Huh-7.5 cells (2×10^5 cells per well in 24-well plates) and incubated in a 5% CO_2 incubator. After 3 hr, the inocula were removed and fresh complete DMEM were added to the cells. At 24 hr postinfection, cells were fixed with ice-cold methanol, blocked with 5% goat serum in phosphate-buffered saline and subjected to immunofluorescence analysis using mouse monoclonal antibody against HCV core antigen (2H9) [Wakita et al., 2005] and Alexa Fluor 488-conjugated goat anti-mouse IgG (H + L) (Molecular Probes, Eugene, OR). The immunostained cells were counterstained with Hoechst 33342 (Molecular Probes) at room temperature for 5 min and observed under a fluorescence microscope (BZ-9000; Keyence, Osaka, Japan). The number of HCV-infected cells in each well was counted by using a software BZ-H1C (Keyence). The serum dilutions that neutralized 50% of the virus infectivity was calculated by curvilinear regression analysis [Abe et al., 2003]. Titers were expressed as 50% neutralization titers (NT_{50}).

Statistical Analysis

Student's *t*-test was used to compare the data between different groups. A *P*-value of <0.05 was considered to be significant.

RESULTS

Anti-HCV Neutralizing Antibodies in Sera of Patients Infected With HCV

Sera were obtained from patients chronically infected with HCV-1b or -2a, and tested for anti-HCV neutralizing activities. Representative results of neutralization curves using the parental J6/JFH1 and the P-47 mutant as challenge viruses are shown in Figure 1. When measured against J6/JFH1, NT_{50} titers of sera of patients infected with HCV-1b ranged from 1:10 to 1:700, with the mean NT_{50} titer being 1:197, whereas those of patients infected with HCV-2a ranged from 1:100 to 1:1,500, with the mean value being 1:670 (Table I). The difference in NT_{50} between patients infected with HCV-1b and -2a was statistically significant ($P < 0.00001$). When measured against P-47, on the other hand, unexpectedly high NT_{50} titers were obtained ranging from 1:4,000 to 1:182,000, with the mean values being 1:40,500 and 1:32,900 for patients infected with HCV-1b and -2a, respectively. These results suggest the possibility that an adaptive mutation(s) of P-47, most probably present in the envelope glycoproteins, confers higher sensitivity to neutralization by anti-HCV antibodies.

Unlike the case with J6/JFH1, when P-47 was used as a challenge virus, no significant difference in NT_{50} titers was observed between patients infected with HCV-1b and -2a (Table I). This result suggests the possible presence of a genotype-dominant neutralization epitope(s) on the envelope glycoproteins of J6/JFH1 although anti-HCV neutralizing antibodies in patients' sera are reactive to both HCV-1b and -2a. The broad reactivity of the neutralizing antibodies in patients' sera across different HCV genotypes is consistent with previous observations by other researchers [Logvinoff et al., 2004; Meunier et al., 2005; Fournier et al., 2007; Pestka et al., 2007; Scheel et al., 2008].

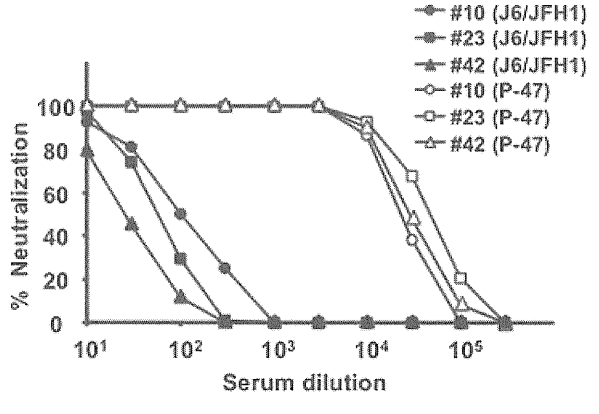

Fig. 1. Neutralization curves (NT_{50} assay) of sera obtained from HCV-infected patients against HCV J6/JFH1 and its adaptive mutant P-47. J6/JFH1 or P-47 was incubated with serial dilutions of HCV-infected patients (nos. 10, 23, and 42; all infected with HCV-1b) and tested for neutralization activities. The neutralization rates at each dilution were plotted. Filled and open symbols indicate data obtained with J6/JFH1 and P-47, respectively.

Sera obtained from patients with acute hepatitis C contained much lower titers of anti-HCV neutralizing antibodies compared to those in sera from chronic hepatitis patients, with the average NT_{50} titers against J6/JFH1 and the adaptive mutant P-47 being 1:15 and 1:126, respectively (Table I). Two patients with severe acute hepatitis C with elevated serum alanine aminotransferase levels of >1,000 IU/ml [Saito et al., 2004; unpublished], possessed relatively high NT_{50} titers against P-47 (1:150 and 1:1,100) compared to the remaining nine patients who experienced mild self-resolving hepatitis (<1:10 to 1:50).

A Single-Point Mutation (N534H or T416A) of the HCV E2 Glycoprotein Increases Sensitivity to Neutralization by Anti-HCV Antibodies

Neutralization of virus infectivity by antibodies usually involves their interaction with viral envelope glycoproteins. It has been reported that the cell culture-adapted mutant P-47 possesses 10 amino acid mutations, including four mutations in E2, compared to the parental J6/JFH1 [Bungyoku et al., 2009]. To examine which mutation(s) in E2 is responsible for the increased sensitivity of P-47 to neutralization by antibodies in patients' sera, recombinant viruses possessing each one of the four mutations in E2 were used (Fig. 2A). The result obtained revealed that a recombinant virus possessing a single-point mutation at position 534 from Asn to His (N534H) and another one possessing four mutations (E2) were as sensitive as P-47 to neutralization by sera of chronic hepatitis patients (Fig. 2B) and the two patients with acute hepatitis C (data not shown). The T416A and T396A mutants were also significantly more sensitive than J6/JFH1, but less sensitive than P-47, N534H, and E2 mutants, to neutralization by antibodies in patients' sera. In this connection, it was recently reported that a JFH1 virus-based T416A mutant showed increased sensitivity to antibody neutralization [Dhillon et al., 2010].

DISCUSSION

The present results revealed that sera of patients infected with HCV-1b possessed cross-genotypic neutralizing antibodies against the J6/JFH1 strain of HCV-2a, albeit with significantly lower titers (ca. one-third) compared to the homotypic neutralization titers observed for patients infected with HCV-2a (Table I). When measured against the adaptive mutant P-47 derived from J6/JFH1, neutralizing antibody titers of the patients sera increased markedly to the level 50- to 200-times higher than that measured against J6/JFH1. Also, the partial genotype-specificity observed with J6/JFH1 was no longer evident when measured against P-47. The marked increase in the sensitivity of P-47 to antibody neutralization was assigned to a mutation at position 534 (N534H), and another one at position 416 (T416A) to a lesser extent, of the E2 glycoprotein (Fig. 2).

TABLE I. NT_{50} Titers in Sera of HCV-Infected Patients With Chronic or Acute Hepatitis C

CH/AH	Genotype	NT_{50} titer[a] measured against J6/JFH1	NT_{50} titer[a] measured against P-47
CH	HCV-1b (n = 69)	197 ± 164 (1)	40,500 ± 31,800 (206)
CH	HCV-2a (n = 20)	670 ± 652[b] (3.4)	32,900 ± 26,500[c] (167)
AH	HCV-1b (n = 11)	15 ± 28 (0.08) (<10–100)	126 ± 326 (0.6) (<10–1,100)

CH, chronic hepatitis; AH, acute hepatitis.
[a]Mean ± SD. The number in the parenthesis means the ratio when compared to the mean titer that was obtained with sera of HCV-1b-infected CH patients against J6/JFH1.
[b]$P < 0.00001$, compared to the mean titer obtained with sera of HCV-1b-infected patients against J6/JFH1 (Student's t-test).
[c]$P = 0.33$, compared to the mean titer obtained with sera of HCV-1b-infected patients against P-47 (Student's t-test).

The N534H and T416A mutations are located at the sixth, and in close proximity to the first, respectively, of the conserved 11 *N*-linked glycosylation sites of the HCV E2 glycoprotein [Helle et al., 2007; Bungyoku et al., 2009]. It was recently reported that the positions 416 and 534 are conformationally located in the former and the latter halves of the central domain 1 (DIa and DIb), respectively, of E2 and that the two parts of DI domain interact to form the CD81-binding region [Helle et al., 2010; Krey et al., 2010; Albecka et al., 2011]. This region is, therefore, considered as the possible target for neutralizing antibodies that inhibit E2-CD81 interactions [Helle and Dubuisson, 2008; Law et al., 2008; Owsianka et al., 2008; Perotti et al., 2008].

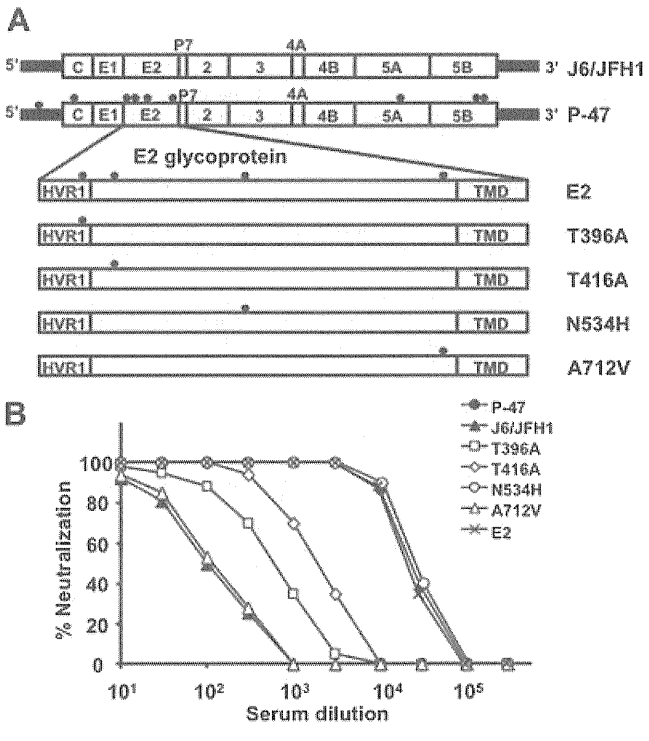

Fig. 2. Effects of amino acid mutations at positions 396, 416, 534, and 712 of the HCV E2 glycoprotein on neutralization by anti-HCV antibodies in patients' sera. **A**: A schematic diagram of the mutations seen in the adaptive mutant P-47 and recombinant viruses carrying each (T396A, T416A, N534H, and A712V) and all (E2) of the four mutations in E2. Filled circles indicate the positions of the mutations. **B**: A representative result of virus neutralization by anti-HCV antibodies in an HCV-infected patient (no. 10; HCV-1b).

The N534H mutation removes glycans at this position as it disrupts the consensus sequence for *N*-linked glycosylation. The removal of glycans at positions 417, 532, and 645 (the first, sixth, and eleventh glycosylation site, respectively) of the H77 isolate (HCV-1a) was shown to increase the sensitivity of HCVpp to neutralizing antibodies and to enhance the access of CD81 to its binding site on E2 [Falkowska et al., 2007; Helle et al., 2007]. It should be noted, however, that the HCVpp system relies on retroviral pseudoparticles bearing HCV envelope glycoproteins that assemble at the plasma membrane or in multivesicular bodies whereas HCV virions assemble on the endoplasmic reticulum membranes that are closely associated with lipid droplet [Miyanari et al., 2007; Helle and Dubuisson, 2008]. Therefore, the virus neutralization data obtained with HCVpp should be verified using the HCVcc system in which virion assembly and maturation take place through the authentic process.

By using the HCVcc system, it was shown that a variant virus possessing the N534K mutation spread faster than the parental JFH1 virus [Delgrange et al., 2007], with the result suggesting the possibility that removal of glycans on residue 534 resulted in more efficient access of E2 to CD81. It is also possible that removal of glycans on this residue might allow more efficient access of neutralizing antibodies to the CD81-binding region of E2, resulting in increased sensitivity to antibody neutralization. In fact, Helle et al. [2010] recently reported that removal of glycans at five (the first, second, fourth, sixth, and eleventh) *N*-linked glycosylation sites in E2 markedly increased the sensitivity of JFH1 virus to antibody neutralization, suggesting that the glycans interfere with the access of neutralizing antibodies to a determinant crucial for virus infectivity. It was also reported that mutations at positions 415 (N415D) and 416 (T416A) near the first glycosylation site of JFH1 virus increased the sensitivity to neutralizing antibodies in patients' sera [Dhillon et al., 2010]. Also, a mutation at position 451 (G451R), which is located in the domain 2 (DII) but still in close proximity to DI [Helle et al., 2010; Krey et al., 2010; Albecka et al., 2011],

increased the sensitivity of JFH1 virus to antibody neutralization [Grove et al., 2008].

In conclusion, the present study using J6/JFH1 virus, another HCVcc strain, has demonstrated that the N534H mutation within the sixth *N*-glycosylation site of the E2 glycoprotein, and the T416A mutation near the first *N*-glycosylation site to a lesser extent, markedly enhances sensitivity to neutralization by antibodies in sera of HCV-infected patients. These results suggest that glycans on Asn-534 of the HCV E2 glycoprotein plays an important role in protecting the virus from humoral immune mechanisms of the host.

ACKNOWLEDGMENTS

We are grateful to Dr. C.M. Rice (Center for the Study of Hepatitis C, the Rockefeller University, New York, NY, USA) for providing pFL-J6/JFH1 and Huh-7.5 cells.

REFERENCES

Abe M, Kuzuhara S, Kino Y. 2003. Establishment of an analyzing method for a Japanese encephalitis virus neutralization test in vero cells. Vaccine 21:1989–1994.

Albecka A, Monserret R, Krey T, Tarr AW, Diesis E, Ball JK, Descamps V, Duverlie G, Rey F, Penin F, Dubuisson J. 2011. Identification of new functional regions in hepatitis C virus envelope glycoprotein E2. J Virol JVI accepts, 85:1777–1792.

Bartosch B, Bukh J, Meunier JC, Granier C, Engle RE, Blackwelder WC, Emerson SU, Cosset FL, Purcell RH. 2003. In vitro assay for neutralizing antibody to hepatitis C virus: Evidence for broadly conserved neutralization epitopes. Proc Natl Acad Sci USA 100:14199–14204.

Blight KJ, McKeating JA, Rice CM. 2002. Highly permissive cell lines for subgenomic and genomic hepatitis C virus RNA replication. J Virol 76:13001–13014.

Bowen DG, Walker CM. 2005. Adaptive immune responses in acute and chronic hepatitis C virus infection. Nature 436:946–952.

Bungyoku Y, Shoji I, Makine T, Adachi T, Hayashida K, Nagano-Fujii M, Ide YH, Deng L, Hotta H. 2009. Efficient production of infectious hepatitis C virus with adaptive mutations in cultured hepatoma cells. J Gen Virol 90:1681–1691.

Delgrange D, Pillez A, Castelain S, Cocquerel L, Rouillé Y, Dubuisson J, Wakita T, Duverlie G, Wychowski C. 2007. Robust production of infectious viral particles in Huh-7 cells by introducing mutations in hepatitis C virus structural proteins. J Gen Virol 88:2495–2503.

Deng L, Adachi T, Kitayama K, Bungyoku Y, Kitazawa S, Ishido S, Shoji I, Hotta H. 2008. Hepatitis C virus infection induces apoptosis through a Bax-triggered, mitochondrion-mediated, caspase 3-dependent pathway. J Virol 82:10375–10385.

Dhillon S, Witteveldt J, Gatherer D, Owsianka AM, Zeisel MB, Zahid MN, Rychłowska M, Foung SK, Baumert TF, Angus AG, Patel AH. 2010. Mutations within a conserved region of the hepatitis C virus glycprotein that influence virus-receptor interaction and sensitivity to neutralizing antibodies. J Virol 84: 5494–5507.

Dowd KA, Netski DM, Wang XH, Cox AL, Ray SC. 2009. Selection pressure from neutralizing antibodies drives sequence evolution during acute infection with hepatitis C virus. Gastroenterology 136:2377–2386.

El-Shamy A, Sasayama M, Nagano-Fujii M, Sasase N, Imoto S, Kim SR, Hotta H. 2007. Prediction of efficient virological response to pegylated interferon/ribavirin combination therapy by NS5A sequences of hepatitis C virus and anti-NS5A antibodies in pretreatment sera. Microbiol Immunol 51:471–482.

El-Shamy A, Nagano-Fujii M, Sasase N, Imoto S, Kim SR, Hotta H. 2008. Sequence variation in hepatitis C virus nonstructural protein 5A predicts clinical outcome of pegylated interferon/ribavirin combination therapy. Hepatology 48:38–47.

Falkowska E, Kajumo F, Garcia E, Reinus J, Dragic T. 2007. Hepatitis C virus envelope glycoprotein E2 glycans modulate entry, CD81 binding, and neutralization. J Virol 81:8072–8079.

Fournier C, Duverlie G, François C, Schnuriger A, Dedeurwaerder S, Brochot E, Capron D, Wychowski C, Thibault V, Castelain S. 2007. A focus reduction neutralization assay for hepatitis C virus neutralizing antibodies. Virol J 4:35.

Gal-Tanamy M, Keck ZY, Yi M, McKeating JA, Patel AH, Foung SK, Lemon SM. 2008. In vitro selection of a neutralization-resistant hepatitis C virus escape mutant. Proc Natl Acad Sci USA 105:19450–19455.

Grove J, Nielsen S, Zhong J, Bassendine MF, Drummer HE, Balfe P, McKeating JA. 2008. Identification of a residue in hepatitis C virus E2 glycoprotein that determines scavenger receptor BI and CD81 receptor dependency and sensitivity to neutralizing antibodies. J Virol 82:12020–12029.

Helle F, Dubuisson J. 2008. Hepatitis C virus entry into host cells. Cell Mol Life Sci 65:100–112.

Helle F, Goffard A, Morel V, Duverlie G, McKeating J, Keck ZY, Foung S, Penin F, Dubuisson J, Voisset C. 2007. The neutralizing activity of anti-hepatitis C virus antibodies is modulated by specific glycans on the E2 envelope protein. J Virol 81:8101–8111.

Helle F, Vieyres G, Elkrief L, Popescu CI, Wychowski C, Descamps V, Castelain S, Roingeard P, Duverlie G, Dubuisson J. 2010. Role of N-linked glycans in the functions of hepatitis C virus envelope proteins incorporated into infectious virions. J Virol 84:11905–11915.

Keck ZY, Olson O, Gal-Tanamy M, Xia J, Patel AH, Dreux M, Cosset FL, Lemon SM, Foung SK. 2008. A point mutation leading to hepatitis C virus escape from neutralization by a monoclonal antibody to a conserved conformational epitope. J Virol 82:6067–6072.

Krey T, d'Alayer J, Kikuti CM, Saulnier A, Damier-Piolle L, Petitpas I, Johansson DX, Tawar RG, Baron B, Robert B, England P, Persson MA, Martin A, Rey FA. 2010. The disulfide bonds in glycoprotein E2 of hepatitis C virus reveal the tertiary organization of the molecule. PLoS Pathog 6:e1000762.

Lavillette D, Morice Y, Germanidis G, Donot P, Soulier A, Pagkalos E, Sakellariou G, Intrator L, Bartosch B, Pawlotsky JM, Cosset FL. 2005. Human serum facilitates hepatitis C virus infection, and neutralizing responses inversely correlate with viral replication kinetics at the acute phase of hepatitis C virus infection. J Virol 79:6023–6034.

Law M, Maruyama T, Lewis J, Giang E, Tarr AW, Stamataki Z, Gastaminza P, Chisari FV, Jones IM, Fox RI, Ball JK, McKeating JA, Kneteman NM, Burton DR. 2008. Broadly neutralizing antibodies protect against hepatitis C virus quasispecies challenge. Nat Med 14:25–27.

Lindenbach BD, Evans MJ, Syder AJ, Wölk B, Tellinghuisen TL, Liu CC, Maruyama T, Hynes RO, Burton DR, McKeating JA, Rice CM. 2005. Complete replication of hepatitis C virus in cell culture. Science 309:623–626.

Logvinoff C, Major ME, Oldach D, Heyward S, Talal A, Balfe P, Feinstone SM, Alter H, Rice CM, McKeating JA. 2004. Neutralizing antibody response during acute and chronic hepatitis C virus infection. Proc Natl Acad Sci USA 101:10149–10154.

Meunier JC, Engle RE, Faulk K, Zhao M, Bartosch B, Alter H, Emerson SU, Cosset FL, Purcell RH, Bukh J. 2005. Evidence for cross-genotype neutralization of hepatitis C virus pseudoparticles and enhancement of infectivity by apolipoprotein C1. Proc Natl Acad Sci USA 102:4560–4565.

Miyanari Y, Atsuzawa K, Usuda N, Watashi K, Hishiki T, Zayas M, Bartenschlager R, Wakita T, Hijikata M, Shimotohno K. 2007. The lipid droplet is an important organelle for hepatitis C virus production. Nat Cell Biol 9:1089–1097.

Netski DM, Mosbruger T, Depla E, Maertens G, Ray SC, Hamilton RG, Roundtree S, Thomas DL, McKeating J, Cox A. 2005. Humoral immune response in acute hepatitis C virus infection. Clin Infect Dis 41:667–675.

Owsianka AM, Tarr AW, Keck ZY, Li TK, Witteveldt J, Adair R, Foung SK, Ball JK, Patel AH. 2008. Broadly neutralizing human monoclonal antibodies to the hepatitis C virus E2 glycoprotein. J Gen Virol 89:653–659.

Perotti M, Mancini N, Diotti RA, Tarr AW, Ball JK, Owsianka A, Adair R, Patel AH, Clementi M, Burioni R. 2008. Identification of a broadly cross-reacting and neutralizing human monoclonal

antibody directed against the hepatitis C virus E2 protein. J Virol 82:1047–1052.

Pestka JM, Zeisel MB, Bläser E, Schürmann P, Bartosch B, Cosset FL, Patel AH, Meisel H, Baumert J, Viazov S, Rispeter K, Blum HE, Roggendorf M, Baumert TF. 2007. Rapid induction of virus-neutralizing antibodies and viral clearance in a single-source outbreak of hepatitis C. Proc Natl Acad Sci USA 104:6025–6030.

Saito T, Watanabe H, Shao L, Okumoto K, Hattori E, Sanjo M, Misawa K, Suzuki A, Takeda T, Sugahara K, Ito JI, Saito K, Togashi H, Kawata S. 2004. Transmission of hepatitis C virus quasispecies between human adults. Hepatol Res 30:57–62.

Sasayama M, Deng L, Kim SR, Ide Y, Shoji I, Hotta H. 2010. Analysis of neutralizing antibodies against hepatitis C virus in patients who were treated with pegylated-interferon plus ribavirin. Kobe J Med Sci 56:E60–E66.

Scheel TK, Gottwein JM, Jensen TB, Prentoe JC, Hoegh AM, Alter HJ, Eugen-Olsen J, Bukh J. 2008. Development of JFH1-based cell culture systems for hepatitis C virus genotype 4a and evidence for cross-genotype neutralization. Proc Natl Acad Sci USA 105:997–1002.

Tarr AW, Owsianka AM, Timms JM, McClure CP, Brown RJ, Hickling TP, Pietschmann T, Bartenschlager R, Patel AH, Ball JK. 2006. Characterization of the hepatitis C virus E2 epitope defined by the broadly neutralizing monoclonal antibody AP33. Hepatology 43:592–601.

Wakita T, Pietschmann T, Kato T, Date T, Miyamoto M, Zhao Z, Murthy K, Habermann A, Kräusslich HG, Mizokami M, Bartenschlager R, Liang TJ. 2005. Production of infectious hepatitis C virus in tissue culture from a cloned viral genome. Nat Med 11:791–796.

Zhong J, Gastaminza P, Cheng G, Kapadia S, Kato T, Burton DR, Wieland SF, Uprichard SL, Wakita T, Chisari FV. 2005. Robust hepatitis C virus infection in vitro. Proc Natl Acad Sci USA 102:9294–9299.

Microbiology and Immunology

Microbiol Immunol 2011; **55**: 418–426
doi:10.1111/j.1348-0421.2011.00331.x

ORIGINAL ARTICLE

Sequence heterogeneity of NS5A and core proteins of hepatitis C virus and virological responses to pegylated-interferon/ribavirin combination therapy

Ahmed El-Shamy[1,2], Ikuo Shoji[1], Takafumi Saito[3], Hisayoshi Watanabe[3], Yoshi-Hiro Ide[1], Lin Deng[1], Sumio Kawata[3] and Hak Hotta[1]

[1]Division of Microbiology, Center for Infectious Diseases, Kobe University Graduate School of Medicine, Kobe, Japan, [2]Department of Virology, Suez Canal University Faculty of Veterinary Medicine, Ismalia, Egypt, and [3]Department of Gastroenterology, Yamagata University School of Medicine, Yamagata, Japan

ABSTRACT

Both host and viral factors have been implicated in influencing the response to pegylated-interferon/ribavirin (PEG-IFN/RBV) therapy for hepatitis C virus (HCV) infection. Among the viral factors, sequence heterogeneity within NS5A and core regions has been proposed. This study aimed to clarify the relationship between virological responses to PEG-IFN/RBV therapy and sequence heterogeneity within NS5A, including the IFN/RBV resistance-determining region (IRRDR), the interferon sensitivity-determining region (ISDR) and the core region. Pretreatment sequences of NS5A and the core regions were analyzed in 57 HCV-1b-infected patients who were to be treated with PEG-IFN/RBV. Of 40 patients infected with HCV having an IRRDR with four or more mutations (IRRDR $\geq$ 4), 28 (70%) patients achieved a sustained virological response (SVR). On the other hand, only 4 (24%) of 17 patients infected with HCV having an IRRDR with three or fewer mutations (IRRDR $\leq$ 3) achieved a SVR ($P = 0.001$). Similarly, 22 (71%) of 31 patients infected with HCV and having an ISDR with one or more mutations (ISDR $\geq$ 1) achieved a SVR while 10 (38%) of 26 patients infected with HCV and having an ISDR without any mutations (ISDR = 0) achieved a SVR ($P = 0.014$). As for the core region, there was significant correlation between a single mutation at position 70 (Gln^{70}) and non-SVR ($P = 0.02$). Notably, Gln^{70} was more prominently associated with the null response ($P = 0.0007$). In conclusion, sequence heterogeneity within the IRRDR and ISDR, and a single point mutation at position 70 of the core region of HCV-1b are likely to be correlated with virological responses to PEG-IFN/RBV therapy.

Key words Core, interferon/ribavirin resistance-determining region, interferon sensitivity-determining region, pegylated-interferon/ribavirin.

Hepatitis C virus is a major cause of chronic liver diseases worldwide. Approximately 180 million people, ~3% of the world's population, are infected with HCV. Seventy percent of acute infections become persistent, and 50–75%

Correspondence
Hak Hotta, Division of Microbiology, Center for Infectious Diseases, Kobe University Graduate School of Medicine, 7-5-1 Kusunoki-cho, Chuo-ku, Kobe 650-0017, Japan.
Tel: +81 78 382 5500; fax: +81 78 382 5519; email: hotta@kobe-u.ac.jp

Received 6 December 2010; revised 31 January 2011; accepted 17 February 2011.

List of Abbreviations: aa, amino acids; Arg^{70}, arginine at position 70 of core protein; AUC, area under the curve; CI, confidence intervals; ETR, end-of-treatment response; EVR, early virological response; Gln^{70}, glutamine at position 70 of core protein; γ-GTP, γ-glutamyl transpeptidase; HCV, hepatitis C virus; IFN, interferon; IRRDR, interferon/ribavirin resistance-determining region; ISDR, interferon sensitivity-determining region; Leu^{91}, leucine at position 91 of core protein; Met^{91}, methionine at position 91 of core protein; NS5A, nonstructural protein 5A; PEG-IFN/RBV, pegylated-interferon/ribavirin; PKR, double-stranded RNA-activated protein kinase; RBV, ribavirin; ROC, receiver operating characteristic; RVR, rapid virological response; SVR, sustained virological response.

of patients with chronic HCV infection progress to hepatocellular carcinoma (1–5). Therefore, HCV infection is a major global health problem. Although more than two decades have passed since the discovery of HCV, therapeutic options remain limited. Current standard treatment of chronic HCV infection consists of PEG-IFN and RBV, which leads to a SVR in approximately half of treated patients, especially those infected with the most resistant genotypes, HCV-1a and HCV-1b (6, 7). Given the considerable side effects and high cost of this treatment, which result in discontinuation of treatment by some patients, reliable prediction of treatment outcome is needed. An expanded range of predictors may assist clinicians and patients to more accurately assess the likelihood of an SVR and thus to make more reliably informed treatment decisions (8).

Because the SVR rate to PEG-IFN/RBV therapy depends on viral genotypes, it is generally considered that HCV genetics affect the treatment response (9). In this context, NS5A has been widely discussed because of its known correlation with IFN responsiveness. Initially, in the era of IFN monotherapy, it was proposed that sequence variations within a region in NS5A spanning from aa 2209 to 2248, called the ISDR, were correlated with IFN responsiveness (10). Subsequently, in the era of combination therapy with PEG-IFN/RBV, we identified a new region near the C-terminus of NS5A spanning from aa 2334 to 2379, which we referred to as the IRRDR (11). The degree of sequence variations within the IRRDR was significantly associated with the clinical outcome of PEG-IFN/RBV combination therapy. On the other hand, prediction of SVR by aa substitutions at positions 70 and 91 of the core protein in Japanese patients infected with HCV-1b has also been proposed (12–14). More recently, we investigated the impact of NS5A polymorphisms, including those in IRRDR and ISDR, and core polymorphism on virological responses to PEG-IFN/RBV therapy among HCV-1b-infected patients in Hyogo Prefecture, Japan. The criterion of six or more mutations in the IRRDR (IRRDR $\geq$ 6) was identified as the most powerful viral genetic factor that independently predicted SVR (15). In another study curried out on a patient cohort in Yamagata Prefecture, Japan, we proposed that polymorphism in the secondary structure of the N-terminal region of NS3 of HCV-1b influences virological responses to PEG-IFN/RBV therapy, and that virus grouping based on NS3 polymorphism can also be used to predict the outcome of the therapy (16). In the present study, we further analyzed the Yamagata cohort for a possible relationship between heterogeneity of NS5A and the core regions of the HCV genome and virological responses to PEG-IFN/RBV therapy.

MATERIALS AND METHODS

Patients

Fifty-seven patients who were chronically infected with HCV-1b, their diagnoses being based on detection of anti-HCV antibody and HCV RNA, and who had been seen at Yamagata University Hospital in Yamagata, Japan, were enrolled in the study. Their HCV subtypes were determined according to the method of Okamoto *et al.* (17). Patients were treated with PEG-IFNα-2b (Pegintron; Schering-Plough, Kenilworth, NJ, USA) (1.5 μg per kilogram of body weight, once weekly, subcutaneously) and RBV (Rebetol; Schering-Plough) (600~800 mg daily, orally), according to a standard treatment protocol for Japanese patients established by a Hepatitis Study Group of the Ministry of Health, Labor and Welfare, Japan. All patients received >80% of the scheduled doses of PEG-IFN and RBV. Serum samples were collected from the patients before treatment and at intervals of 4 weeks during the whole observation period (72 weeks), and tested for HCV RNA titers as reported previously (18).

The study protocol was approved beforehand by the Ethics Committee at Yamagata University Hospital, and written informed consent for study participation was obtained from each patient prior to treatment. Also, the study protocol conforms to the provisions of the Declaration of Helsinki.

Sequence analysis of hepatitis C virus NS5A and the core regions of the hepatitis C virus genome

Hepatitis C virus RNA was extracted from 140 μL of serum using a commercially available kit (QIAmp viral RNA kit; Qiagen, Tokyo, Japan). Amplification of full-length NS5A and the core regions of the HCV genome were performed as described elsewhere (11, 18, 19). The sequences of the amplified fragments of NS5A and core regions were determined by direct sequencing without subcloning. The aa sequences were deduced and aligned using GENETYX Win software version 7.0 (Genetyx, Tokyo, Japan).

Statistical analysis

To evaluate the optimal threshold of the IRRDR and ISDR mutations for SVR prediction, we constructed an ROC curve and calculated the AUC, sensitivity and specificity (11). Statistical differences in treatment responses according to NS5A and core sequence heterogeneity were determined by the χ^2 test. Likewise, statistical differences in the patients' baseline variables according to the degree of IRRDR polymorphism were determined by Student's *t*

test for numerical variables and the χ^2 probability test for categorical variables. Univariate and multivariate logistic analyses were performed to identify variables that were independently correlated with the treatment outcome. Variables with a P value of <0.1 in univariate analysis were further included in a multivariate logistic regression analysis. The odds ratios and 95% CI were also calculated. All statistical analyses were performed using SPSS version 16 software (SPSS, Chicago, IL, USA). Unless otherwise stated, a P value of <0.05 was considered statistically significant.

Nucleotide sequence accession numbers

The sequence data reported in this paper have been deposited in the DDBJ/EMBL/GenBank nucleotide sequence databases under the accession numbers AB601987 through AB602043.

RESULTS

Patients' responses to pegylated-interferon/ribavirin combination therapy

Among the 57 patients enrolled in this study, 8 (14%), 36 (63%), 42 (74%) and 32 (56%) patients were negative for HCV-RNA at week 4 (RVR), week 12 (EVR), week 48 (ETR) and week 72 (SVR), respectively (Table 1). SVR was achieved by all (100%) of RVR, 30 (83%) of 36 EVR, and 32 (76%) of 42 ETR patients. Non-SVR patients represented 44% (25/57) of total cases. Twenty-six percent (15/57) of the patients had continuous viremia during the whole observation period (72 weeks), referred to as a null response; whereas 18% (10/57) had transient disappearance of serum HCV RNA at a certain time point followed by a rebound in viremia either before, or after the end of, the treatment course, referred to as a relapse.

Table 1. Proportions of various virological responses of patients treated with PEG-IFN/RBV

Virological response	Proportion
RVR	14% (8/57)†
EVR	63% (36/57)
ETR	74% (42/57)
SVR	56% (32/57)
Non-SVR	44% (25/57)
Null response	26% (15/57)
Relapse	18% (10/57)

†, number of patients in the relevant category /total number of patients.

Correlation between interferon/ribavirin resistance-determining region polymorphism and treatment responses

The degree of sequence variation within the IRRDR has been proposed as a useful predictor of HCV treatment outcome (11, 15, 20, 21). We performed ROC curve analysis to estimate the optimal cutoff number of IRRDR mutations that differentiated between a SVR and non-SVR in the present patient cohort. Based on the results obtained, we estimated four mutations as the optimal number of IRRDR mutations since this provided the highest sensitivity (88%) and good specificity (52%) with an

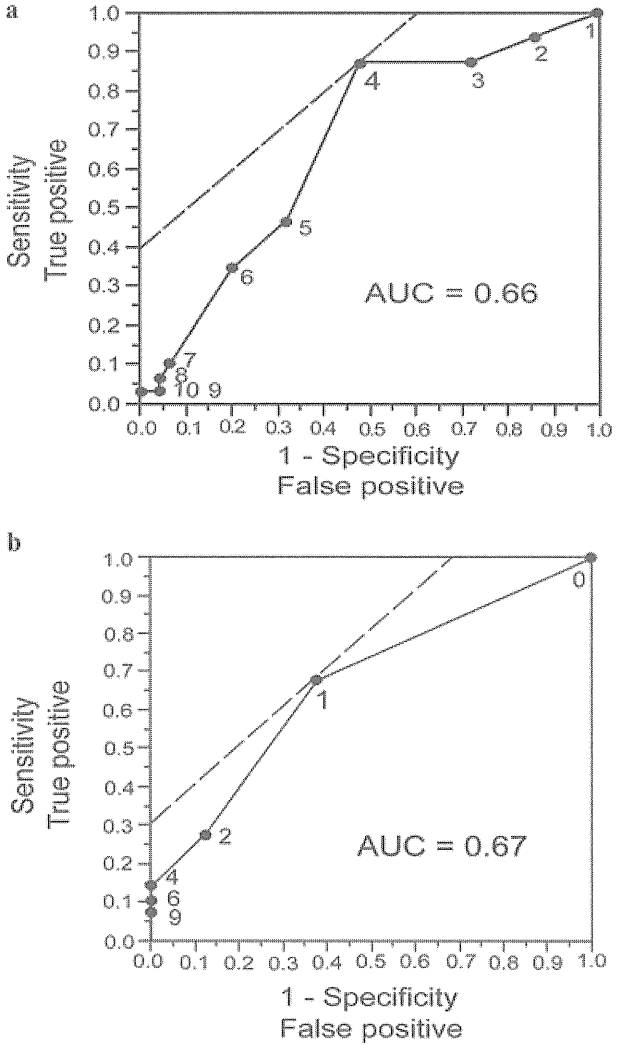

Fig. 1. ROC curve analysis of (a) IRRDR and (b) ISDR sequence heterogeneity for SVR prediction. The curves depicted by solid lines shows the AUC. Solid circles with numerals plotted on the curve represent different numbers of IRRDR and ISDR mutations analyzed. The dashed lines touch the optimal number of IRRDR and ISDR mutations for SVR prediction.

Table 2. Correlation between NS5A and core protein polymorphisms and virological responses of patients treated with PEG-IFN/RBV

Protein	Factor	Total †	SVR ‡	Non-SVR	Null response	Relapse	*P* value		
							SVR vs non-SVR	SVR vs null response	SVR vs relapse
NS5A	IRRDR ≥ 4	40	28 (70%)	12 (30%)	7 (17.5%)	5 (12.5%)	**0.001**	**0.003**	**0.01**
	IRRDR ≤ 3	17	4 (24%)	13 (76%)	8 (47%)	5 (29%)			
	ISDR ≥ 1	31	22 (71%)	9 (29%)	5 (16%)	4 (13%)	**0.014**	**0.02**	0.1
	ISDR = 0	26	10 (38%)	16 (62%)	10 (38%)	6 (24%)			
Core	Wild-core (Arg^{70}/Leu^{91})	24	15 (63%)	9 (37%)	5 (21%)	4 (16%)	0.4	0.4	0.7
	Non-wild-core	33	17 (52%)	16 (48%)	10 (30%)	6 (18%)			
	Gln^{70}	14	4 (29%)	10 (71%)	9 (64%)	1 (7%)	**0.02**	**0.0007**	0.8
	Non- Gln^{70}	43	28 (65%)	15 (35%)	6 (14%)	9 (21%)			
	Met^{91}	22	10 (46%)	12 (54%)	6 (27%)	6 (27%)	0.2	0.6	0.1
	Non- Met^{91}	35	22 (63%)	13 (37%)	9 (26%)	4 (11%)			

†, total number of isolates with a given factor; ‡, number of SVR, non-SVR, null-response or relapse cases with a given factor. *P* values indicating statistically significant difference are written in bold.

AUC of 0.66 (Fig. 1a). In this study, therefore, we used the criteria of four or more mutations in the IRRDR (IRRDR ≥ 4) and IRRDR ≤ 3. In this connection, it should be stated that the criteria of IRRDR ≥ 6 and IRRDR ≤ 5 which were used on different patient cohorts in Hyogo Prefecture (11, 15) were not selected by the ROC curve analysis in this study because of their low sensitivity (34%), although they had higher specificity (80%) than that of IRRDR ≥ 4 (52%). This difference was probably due to the low prevalence of HCV isolates with IRRDR ≥ 6 (28%) in the present patient cohort.

We found that 70%, 30%, 17.5% and 12.5% of patients infected with HCV isolates with IRRDR ≥ 4 were SVR, non-SVR, null response and relapse cases, respectively (Table 2 and Fig. 2). By contrast, 24%, 76%, 47% and 29% of patients infected with HCV isolates with IRRDR ≤ 3 were SVR, non-SVR, null response and relapse cases, respectively. Thus, the proportions of SVR, non-SVR, null response and relapse cases were significantly different among HCV isolates with IRRDR ≥ 4 and IRRDR ≤ 3.

Interestingly, while IRRDR polymorphism was correlated with the final treatment outcome, it was also closely correlated with all the responses during treatment, represented by RVR, EVR and ETR (Table 3).

Next, we investigated the correlations between the patients' demographic, hematological, biochemical and virological baseline variables and the degree of IRRDR polymorphism. This analysis revealed that patient age was the only factor that was significantly correlated with the degree of IRRDR polymorphism, patients who were infected with HCV isolates of IRRDR ≥ 4 being significantly younger on average than patients infected with HCV isolates with IRRDR ≤ 3 ($P = 0.035$) (Table 4).

Correlation between interferon sensitivity-determining region polymorphism and treatment responses

Based on ROC curve analysis, we estimated one mutation in the ISDR as an optimal cut-off number of mutations for SVR prediction since it had the highest sensitivity (69%) combined with the highest specificity (64%) and yielded an AUC of 0.67 (Fig. 1b). Seventy-one percent, 29%, 16% and 13% of patients infected with HCV isolates with one or more mutations in the ISDR (ISDR ≥ 1) were SVR, non-SVR, null response and relapse cases, respectively (Table 2 and Fig. 2). By contrast, 38%, 62%, 38% and 24% of patients infected with HCV isolates with no mutation in the ISDR (ISDR = 0) were SVR, non-SVR, null response and relapse cases, respectively. Thus, the proportions of SVR, non-SVR and null response cases were significantly different among HCV isolates with ISDR ≥ 1 and ISDR = 0.

ISDR polymorphism and the on-treatment responses had significant correlation only with EVR, since 77% of patients infected with HCV isolates with ISDR ≥ 1 were EVR whereas 54% of patients infected with HCV isolates with ISDR = 0 were non-EVR ($P = 0.01$, Table 3).

Correlation between core polymorphism and treatment responses

Recently, it was reported that polymorphism at positions 70 and/or 91 of the core protein of HCV-1b are useful negative markers for the treatment outcome of Japanese patients treated with PEG-IFN/RBV combination therapy (12–14). We have investigated the impact of various sequences patterns of both positions on treatment responses. We found that 63%, 37%, 21% and 16%

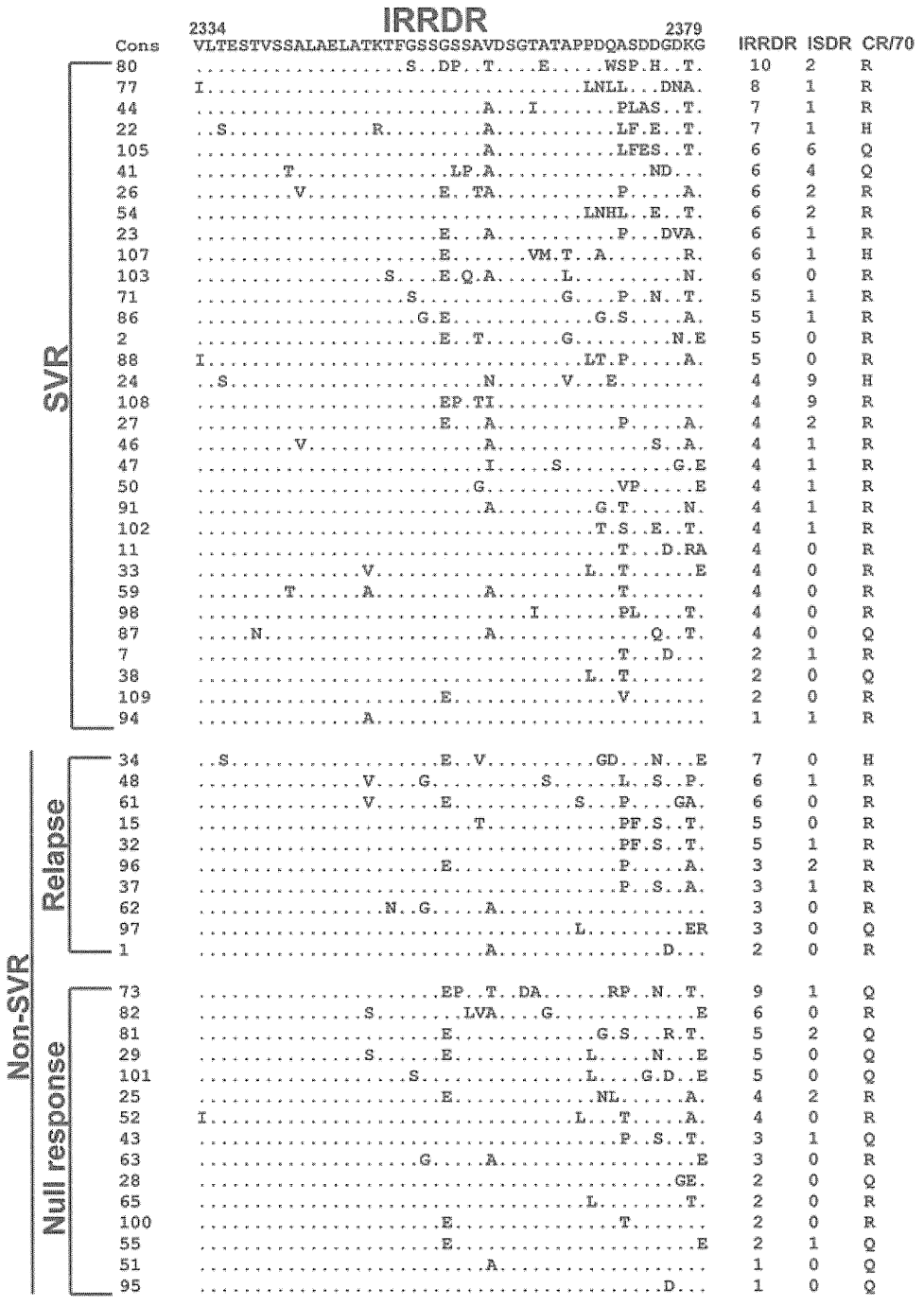

Fig. 2. Sequence alignment of IRRDR of NS5A of HCV-1b obtained from pretreatment sera. The consensus sequence is shown at the top (Cons). Dots indicate residues identical to those of the consensus sequence. Number of IRRDR and ISDR mutations, as well as the sequence pattern at aa 70 of the core protein, are shown on the right. The number of ISDR mutations was determined by comparing with the consensus sequence reported by Enomoto *et al.* (10).

of patients infected with HCV isolates with wild-core (Arg^{70}/Leu^{91}) were SVR, non-SVR, null response and relapse cases, respectively, compared to 52%, 48%, 30% and 18% of patients infected with HCV isolates with non-wild-core (Table 2). Thus, there was no significant correlation between wild-core and SVR or non-SVR ($P = 0.4$). However, the presence of a single point mutation at position 70 (Gln^{70} vs non- Gln^{70}) was significantly associated with

Table 3. Correlation between NS5A and core protein polymorphisms and on-treatment virological responses of patients treated with PEG-IFN/RBV

Protein	Factor	Total †	RVR‡	Non-RVR	EVR	Non-EVR	ETR	Non-ETR	*P* value		
									RVR vs non-RVR	EVR vs non-EVR	ETR versus non-ETR
NS5A	IRRDR ≥ 4	40	8 (20%)	32 (80%)	30 (75%)	10 (25%)	33 (83%)	7 (17%)	**0.047**	**0.005**	**0.02**
	IRRDR ≤ 3	17	0 (0.0%)	17 (100%)	6 (35%)	11 (65%)	9 (53%)	8 (47%)			
	ISDR ≥ 1	31	5 (16%)	26 (84%)	24 (77%)	7 (23%)	26 (84%)	5 (16%)	0.62	**0.01**	0.057
	ISDR = 0	26	3 (12%)	23 (88%)	12 (46%)	14 (54%)	16 (62%)	10 (38%)			
Core	Wild-core (Arg^{70}/Leu^{91})	24	4 (17%)	20 (83%)	17 (71%)	7 (29%)	19 (79%)	5 (21%)	0.63	0.31	0.42
	Non-wild-core	33	4 (12%)	29 (88%)	19 (58%)	14 (42%)	23 (70%)	10 (30%)			
	Gln^{70}	14	2 (14%)	12 (86%)	4 (29%)	10 (71%)	5 (36%)	9 (64%)	0.97	**0.002**	**0.0002**
	Non- Gln^{70}	43	6 (14%)	37 (86%)	32 (74%)	11 (26%)	37 (86%)	6 (14%)			
	Met^{91}	22	1 (5%)	21 (95%)	12 (54%)	10 (46%)	16 (73%)	6 (27%)	0.1	0.29	0.9
	Non- Met^{91}	35	7 (20%)	28 (80%)	24 (69%)	11 (31%)	26 (74%)	9 (26%)			

†, total number of isolates with a given factor; ‡, number of RVR, non-RVR, EVR, non-EVR, ETR or non-ETR cases with a given factor. *P* values indicating statistically significant difference are written in bold.

Table 4. Correlation between IRRDR polymorphism and patients' demographic characteristics

Factor	IRRDR ≥ 4	IRRDR ≤ 3	*P* value
Age	54.1 ± 9.5†	59.2 ± 6.9	**0.035**
Sex (male/female)	23/17	11/6	0.61
Body weight (Kg)	62.4 ± 18.8	64.2 ± 12.1	0.68
Platelets ($\times 10^4/mm^3$)	17.0 ± 5.0	17.7 ± 5.0	0.66
Hemoglobin (g/dl)	14.3 ± 1.2	14.7 ± 1.1	0.21
Neutrophil count	2303 ± 822	2432 ± 658	0.57
γ-GTP (IU/L)	52.6 ± 42.3	80.7 ± 70.5	0.15
Glutamate pyruvate transaminase (IU/L)	80.2 ± 60.7	101.6 ± 79.7	0.33
HCV-RNA (KIU/mL)	1719 ± 1298	2273 ± 1571	0.21

†, mean ± S.D. *P* values indicating statistically significant difference are written in bold.

either a non-SVR or null-response (Table 2 and Fig. 2). Gln^{70} was also the only factor of core protein that was strongly associated with non-EVR and non-ETR responses (Table 3).

Identification of independent viral factors that are significantly correlated with virological responses to pegylated-interferon/ribavirin therapy

In order to identify which independent viral factors are significantly correlated with final and on-treatment responses to PEG-IFN/RBV therapy, data including all available baseline patient variables, NS5A and core polymorphic factors, and previously published data on polymorphism in an N-terminus of NS3 of the same patient cohort (16) were analyzed by univariate and multivariate logistic regression analyses (Table 5). In regard to the final treatment responses, IRRDR ≥ 4 and group A of the N-terminus of NS3 were identified as independent viral factors that are significantly associated with a SVR, whereas IRRDR ≤ 3 and Gln^{70} of core were identified as independent factors associated with a null response. Regarding on-treatment responses, IRRDR ≥ 4 and non-Gln^{70} were identified as independent factors associated with an EVR and ETR.

DISCUSSION

Pegylated-interferon/ribavirin combination therapy has been used to treat chronic HCV infection, the treatment outcome being thought to be affected by both host and viral factors. Recently, IL28B, which encodes IFNλ3, was identified as the major host factor that determines the treatment outcome (22–24). As for the viral factor(s), we and other research groups have reported that

Table 5. Univariate and multivariate logistic regression analyses to identify independent factors significantly associated with virological responses to PEG-IFN/RBV therapy

	Univariate		Multivariate	
Response	Variable	*P* value	Odds ratio (95% CI)	*P* value
SVR	**IRRDR ≥ 4**	0.003	5.2 (1.3–20.1)	**0.02**
	ISDR ≥ 1	0.013		
	Non-Gln^{70}	0.016		
	NS3 / A group	0.013	4.2 (1.0–18.3)	**0.05**
	Viral load	0.04		
Null response	**IRRDR ≤ 3**	0.001	0.2 (0.04–0.7)	**0.02**
	ISDR = 0	0.06		
	Gln^{70}	0.0001	7.8 (1.7–35.5)	**0.008**
	Viral load	0.08		
	NS3 / non-A group	0.03		
	Hemoglobin	0.02		
	γ-GTP	0.08		
Relapse	**Age**	0.02	1.2 (1.0–1.3)	**0.03**
	Sex	0.004		
	Hemoglobin	0.03		
RVR	IRRDR ≥ 4	0.05		
	Hemoglobin	0.02	0.4 (0.2–0.9)	**0.03**
EVR	**IRRDR ≥ 4**	0.001	7.0 (1.6–29.8)	**0.009**
	ISDR≥1	0.01		
	Non-Gln^{70}	0.002	0.2 (0.04–0.8)	**0.02**
	NS3 / A group	0.07		
	Viral load	0.015		
	Hemoglobin	0.07		
	γ-GTP	0.09		
ETR	**IRRDR≥4**	0.001	6.2 (1.4–27.7)	**0.02**
	ISDR≥1	0.06		
	Non-Gln^{70}	0.0001	0.1 (0.03–0.6)	**0.008**
	NS3 / A group	0.03		
	Viral load	0.08		
	Hemoglobin	0.02		
	γ-GTP	0.08		

Variables that were shown by multivariate analysis to be significantly correlated with a certain treatment response are written in bold.

heterogeneity of NS5A and the core proteins of HCV-1b are correlated with treatment outcome (11–15). Furthermore, we recently reported that polymorphism in an N-terminus of NS3 is significantly correlated with virological responses to PEG-IFN/RBV therapy (16). In the present study, we have further expanded the previous study by analyzing possible correlations between heterogeneity of NS5A and the core regions of the HCV-1b genome and virological responses to PEG-IFN/RBV therapy. The present study showed that final and on-treatment responses of patients in the same cohort were also significantly influenced by IRRDR ≥ 4, ISDR ≥ 1 of NS5A, and Gln^{70} of the core protein.

We previously reported IRRDR ≥ 6 as an independent viral factor significantly associated with SVR in different patient cohorts in Hyogo Prefecture (11, 15). Also, ISDR ≥ 2 was identified as the optimal threshold for SVR prediction (20, 25–27). However, in the present study IRRDR ≥ 6 or ISDR ≥ 2 did not correlate significantly with a SVR, although there was a trend toward SVR in these criteria (11 of 16 isolates with IRRDR ≥ 6 and 8 of 11 isolates with ISDR ≥ 2 were obtained from SVR patients). This difference might be attributable to the low prevalence of IRRDR ≥ 6 (16/57) and ISDR ≥ 2 (13/57) in the present patient cohort. Accordingly, in this study the IRRDR and ISDR sequences of the HCV isolates were less variable than were those of other studies. It thus appears that the prevalence of HCV isolates of IRRDR ≥ 6 and ISDR ≥ 2 varies from one geographical region to another. This implies the possibility that certain characteristics of HCV isolates, including IFN sensitivity, may also vary from one geographical region to another. Analysis in a large-scale multicenter study is needed to clarify this possibility.

The NS5A- interferon sensitivity-determining region was first identified to be significantly correlated with the probability of a SVR during the era of IFN monotherapy (10). In the more recent era of combination therapy with PEG-IFN/RBV, the NS5A-IRRDR has been identified to be closely associated with a SVR (11). The ISDR interacts with PKR and regulates replication of HCV *in vitro* (28). Mutations in the ISDR affect the interaction with PKR and may inhibit viral replication. In the case of the IRRDR, the molecular mechanism underlying the possible involvement of this region in IFN responsiveness of the virus is still unknown. The significant difference among IRRDR sequence patterns may suggest genetic flexibility of this region. Thus, changes in the IRRDR might be capable of modulating intracellular antiviral activity, or maybe the genetic flexibility of this region is accompanied by compensatory changes elsewhere in the viral genome and these compensatory changes affect overall viral fitness and responses to IFN therapy (29–31)

When we investigated the impact of various sequences patterns at positions 70 and 91 of the core protein, we observed that single point mutation at position 70 (Gln^{70} vs non-Gln^{70}) was the only factor that significantly influenced treatment responses. This result is consistent with recent reports, including a recent multi-center study in Japan that identified Gln^{70} as a predictive factor for poor responses to PEG-IFN/RBV treatment (14, 13, 30). The core region of HCV interacts with several host factors and modulates expression of numerous genes, including down-regulating IFN-induced antiviral genes, thus inhibiting the antiviral action of IFN (32, 33). Therefore, it would also be interesting to investigate the impact of

polymorphism, both at position 70 and of NS5A, on HCV pathogenesis and IFN sensitivity.

Multivariate logistic regression analysis of all available data, including those of NS5A and core polymorphisms in this study and the data on NS3 polymorphism in the same patient cohort published elsewhere (16), identified IRRDR $\geq$ 4 and group A of NS3 as independent viral factors that are significantly associated with a SVR, and IRRDR $\leq$ 3, and Gln^{70} of the core protein as independent factors significantly associated with a null response (Table 5). No combinations of these criteria produced a more significant correlation with virological responses to PEG-IFN/RBV therapy (data not shown).

In conclusion, the present results demonstrate that sequence heterogeneity of NS5A, especially in IRRDR and ISDR, and a single-point mutation at position 70 of the core protein of HCV-1b are significantly correlated with virological responses to PEG-IFN/RBV therapy. Also, the results emphasize the possible functional importance of NS5A and core protein in regulating viral responsiveness to PEG-IFN/RBV.

ACKNOWLEGMENTS

This study was supported in part by Health and Labor Sciences Research Grants from the Ministry of Health, Labor and Welfare, Japan, and a Science and Technology Research Partnership for Sustainable Development grant from the Japan Science and Technology Agency and Japan International Cooperation Agency. This study was also carried out as part of the Japan Initiative for Global Research Network on Infectious Diseases, Ministry of Education, Culture, Sports, Science and Technology, Japan, and the Global Center of Excellence Program at Kobe University Graduate School of Medicine.

REFERENCES

1. Amoroso P., Rapicetta M., Tosti M.E., Mele A., Spada E., Buonocore S., Lettieri G., Pierri P., Chionne P., Ciccaglione A.R., Sagliocca L. (1998) Correlation between virus genotype and chronicity rate in acute hepatitis C. *J Hepatol* **28**: 939–44.
2. Tanaka E., Kiyosawa K. (2000) Natural history of acute hepatitis C. *J Gastroenterol Hepatol* **15**(Suppl): E97–104.
3. Maekawa S., Enomoto N. (2009) Viral factors influencing the response to the combination therapy of peginterferon plus ribavirin in chronic hepatitis C. *J Gastroenterol* **44**: 1009–15.
4. Mattsson L., Sonnerborg A., Weiland O. (1993) Outcome of acute symptomatic non-A, non-B hepatitis: a 13-year follow-up study of hepatitis C virus markers. *Liver* **13**: 274–8.
5. Micallef J.M., Kaldor J.M., Dore G.J. (2006) Spontaneous viral clearance following acute hepatitis C infection: a systematic review of longitudinal studies. *J Viral Hepat* **13**: 34–41.
6. Fried M.W., Shiffman M.L., Reddy K.R., Smith C., Marinos G., Goncales F.L. Jr., Haussinger D., Diago M., Carosi G., Dhumeaux D., Craxi A., Lin A., Hoffman J., Yu J. (2002) Peginterferon alfa-2a plus ribavirin for chronic hepatitis C virus infection. *N Engl J Med* **347**: 975–82.
7. Sarasin-Filipowicz M. (2009) Interferon therapy of hepatitis C: molecular insights into success and failure. *Swiss Med Wkly* **140**: 3–11
8. Backus L.I., Boothroyd D.B., Phillips B.R., Mole L.A. (2007) Predictors of response of US veterans to treatment for the hepatitis C virus. *Hepatology* **46**: 37–47.
9. Enomoto N., Maekawa S. (2010) HCV genetic elements determining the early response to peginterferon and ribavirin therapy. *Intervirology* **53**: 66–9.
10. Enomoto N., Sakuma I., Asahina Y., Kurosaki M., Murakami T., Yamamoto C., Ogura Y., Izumi N., Marumo F., Sato C. (1996) Mutations in the nonstructural protein 5A gene and response to interferon in patients with chronic hepatitis C virus 1b infection. *N Engl J Med* **334**: 77–81.
11. El-Shamy A., Nagano-Fujii M., Sasase N., Imoto S., Kim S.R., Hotta H. (2008) Sequence variation in hepatitis C virus nonstructural protein 5A predicts clinical outcome of pegylated interferon/ribavirin combination therapy. *Hepatology* **48**: 38–47.
12. Akuta N., Suzuki F., Kawamura Y., Yatsuji H., Sezaki H., Suzuki Y., Hosaka T., Kobayashi M., Kobayashi M., Arase Y., Ikeda K., Miyakawa Y., Kumada H. (2007) Prediction of response to pegylated interferon and ribavirin in hepatitis C by polymorphisms in the viral core protein and very early dynamics of viremia. *Intervirology* **50**: 361–8.
13. Akuta N., Suzuki F., Sezaki H., Suzuki Y., Hosaka T., Someya T., Kobayashi M., Saitoh S., Watahiki S., Sato J., Matsuda M., Kobayashi M., Arase Y., Ikeda K., Kumada H. (2005) Association of amino acid substitution pattern in core protein of hepatitis C virus genotype 1b high viral load and non-virological response to interferon-ribavirin combination therapy. *Intervirology* **48**: 372–80.
14. Akuta N., Suzuki F., Kawamura Y., Yatsuji H., Sezaki H., Suzuki Y., Hosaka T., Kobayashi M., Kobayashi M., Arase Y., Ikeda K., Kumada H. (2007) Predictive factors of early and sustained responses to peginterferon plus ribavirin combination therapy in Japanese patients infected with hepatitis C virus genotype 1b: Amino acid substitutions in the core region and low-density lipoprotein cholesterol levels. *J Hepatol* **46**: 403–10.
15. El-Shamy A., Kim S.R., Ide Y.H., Sasase N., Imoto S., Deng L., Shoji I., Hotta H. (2011) Polymorphisms of hepatitis C virus non-structural protein 5A and core proteins and clinical outcome of pegylated-interferon/ribavirin combination therapy. *Intervirology* (in press).
16. Sanjo M., Saito T., Ishii R., Nishise Y., Haga H., Okumoto K., Ito J., Watanabe H., Saito K., Togashi H., Fukuda K., Imai Y., El-Shamy A., Deng L., Shoji I., Hotta H., Kawata S. (2010) Secondary structure of the amino-terminal region of HCV NS3 and virological response to pegylated interferon plus ribavirin therapy for chronic hepatitis C. *J Med Virol* **82**: 1364–70.
17. Okamoto H., Sugiyama Y., Okada S., Kurai K., Akahane Y., Sugai Y., Tanaka T., Sato K., Tsuda F., Miyakawa Y., Mayumi M. (1992) Typing hepatitis C virus by polymerase chain reaction with type-specific primers: application to clinical surveys and tracing infectious sources. *J Gen Virol* **73**(Pt 3): 673–9.
18. El-Shamy A., Sasayama M., Nagano-Fujii M., Sasase N., Imoto S., Kim S.R., Hotta H. (2007) Prediction of efficient virological response to pegylated interferon/ribavirin combination therapy by NS5A sequences of hepatitis C virus and anti-NS5A antibodies in pre-treatment sera. *Microbiol Immunol* **51**: 471–82.
19. Ogata S., Nagano-Fujii M., Ku Y., Yoon S., Hotta H. (2002) Comparative sequence analysis of the core protein and its

frameshift product, the F protein, of hepatitis C virus subtype 1b strains obtained from patients with and without hepatocellular carcinoma. *J Clin Microbiol* **40**: 3625–30.
20. Fukuhara T., Taketomi A., Okano S., Ikegami T., Soejima Y., Shirabe K., Maehara Y. (2010) Mutations in hepatitis C virus genotype 1b and the sensitivity of interferon-ribavirin therapy after liver transplantation. *J Hepatol* **52**: 672–680.
21. Sasase N., Kim S.R., Kudo M., Kim K.I., Taniguchi M., Imoto S., Mita K., Hayashi Y., Shoji I., El-Shamy A., Hotta H. (2010) Outcome and early viral dynamics with viral mutation in PEG-IFN/RBV therapy for chronic hepatitis in patients with high viral loads of serum HCV RNA genotype 1b. *Intervirology* **53**: 49–54.
22. Ge D., Fellay J., Thompson A.J., Simon J.S., Shianna K.V., Urban T.J., Heinzen E.L., Qiu P., Bertelsen A.H., Muir A.J., Sulkowski M., Mchutchison J.G., Goldstein D.B. (2009) Genetic variation in IL28B predicts hepatitis C treatment-induced viral clearance. *Nature* **461**: 399–401.
23. Suppiah V., Moldovan M., Ahlenstiel G., Berg T., Weltman M., Abate M.L., Bassendine M., Spengler U., Dore G.J., Powell E., Riordan S., Sheridan D., Smedile A., Fragomeli V., Muller T., Bahlo M., Stewart G.J., Booth D.R., George J. (2009) IL28B is associated with response to chronic hepatitis C interferon-alpha and ribavirin therapy. *Nat Genet* **41**: 1100–4.
24. Tanaka Y., Nishida N., Sugiyama M., Kurosaki M., Matsuura K., Sakamoto N., Nakagawa M., Korenaga M., Hino K., Hige S., Ito Y., Mita E., Tanaka E., Mochida S., Murawaki Y., Honda M., Sakai A., Hiasa Y., Nishiguchi S., Koike A., Sakaida I., Imamura M., Ito K., Yano K., Masaki N., Sugauchi F., Izumi N., Tokunaga K., Mizokami M. (2009) Genome-wide association of IL28B with response to pegylated interferon-alpha and ribavirin therapy for chronic hepatitis C. *Nat Genet* **41**: 1105–9.
25. Shirakawa H., Matsumoto A., Joshita S., Komatsu M., Tanaka N., Umemura T., Ichijo T., Yoshizawa K., Kiyosawa K., Tanaka E. (2008) Pretreatment prediction of virological response to peginterferon plus ribavirin therapy in chronic hepatitis C patients using viral and host factors. *Hepatology* **48**: 1753–60.
26. Okanoue T., Itoh Y., Hashimoto H., Yasui K., Minami M., Takehara T., Tanaka E., Onji M., Toyota J., Chayama K., Yoshioka K., Izumi N., Akuta N., Kumada H. (2009) Predictive values of amino acid sequences of the core and NS5A regions in antiviral therapy for hepatitis C: a Japanese multi-center study. *J Gastroenterol* **44**: 952–63.
27. Hayashi K., Katano Y., Ishigami M., Itoh A., Hirooka Y., Nakano I., Urano F., Yoshioka K., Toyoda H., Kumada T., Goto H. (2011) Mutations in the core and NS5A region of hepatitis C virus genotype 1b and correlation with response to pegylated-interferon-alpha 2b and ribavirin combination therapy. *J Viral Hepat* **18**: 280–86
28. Gale M. Jr., Blakely C.M., Kwieciszewski B., Tan S.L., Dossett M., Tang N.M., Korth M.J., Polyak S.J., Gretch D.R., Katze M.G. (1998) Control of PKR protein kinase by hepatitis C virus nonstructural 5A protein: molecular mechanisms of kinase regulation. *Mol Cell Biol* **18**: 5208–18.
29. Moradpour D., Evans M.J., Gosert R., Yuan Z., Blum H.E., Goff S.P., Lindenbach B.D., Rice C.M. (2004) Insertion of green fluorescent protein into nonstructural protein 5A allows direct visualization of functional hepatitis C virus replication complexes. *J Virol* **78**: 7400–9.
30. Appel N., Pietschmann T., Bartenschlager R. (2005) Mutational analysis of hepatitis C virus nonstructural protein 5A: potential role of differential phosphorylation in RNA replication and identification of a genetically flexible domain. *J Virol* **79**: 3187–94.
31. Yuan H.J., Jain M., Snow K.K., Gale M. Jr., Lee W.M. (2009) Evolution of hepatitis C virus NS5A region in breakthrough patients during pegylated interferon and ribavirin therapy. *J Viral Hepat* **17**: 208–216.
32. Bode J.G., Ludwig S., Ehrhardt C., Albrecht U., Erhardt A., Schaper F., Heinrich P.C., Haussinger D. (2003) IFN-alpha antagonistic activity of HCV core protein involves induction of suppressor of cytokine signaling-3. *Faseb J* **17**: 488–90.
33. De Lucas S., Bartolome J., Carreno V. (2005) Hepatitis C virus core protein down-regulates transcription of interferon-induced antiviral genes. *J Infect Dis* **191**: 93–99.

JOURNAL OF VIROLOGY, Sept. 2011, p. 8556–8568 Vol. 85, No. 17
0022-538X/11/$12.00 doi:10.1128/JVI.00146-11

Hepatitis C Virus Infection Promotes Hepatic Gluconeogenesis through an NS5A-Mediated, FoxO1-Dependent Pathway[▽]

Lin Deng,[1] Ikuo Shoji,[1] Wataru Ogawa,[2] Shusaku Kaneda,[1] Tomoyoshi Soga,[3] Da-peng Jiang,[1] Yoshi-Hiro Ide,[1] and Hak Hotta[1]*

Division of Microbiology, Center for Infectious Diseases,[1] and Division of Diabetes, Metabolism and Endocrinology,[2] Kobe University Graduate School of Medicine, 7-5-1 Kusunoki-cho, Chuo-ku, Kobe 650-0017, Japan, and Institute for Advanced Biosciences, Keio University, 246-2 Mizukami, Kakuganji, Tsuruoka, Yamagata 997-0052, Japan[3]

Received 21 January 2011/Accepted 7 June 2011

Chronic hepatitis C virus (HCV) infection is often associated with type 2 diabetes. However, the precise mechanism underlying this association is still unclear. Here, using Huh-7.5 cells either harboring HCV-1b RNA replicons or infected with HCV-2a, we showed that HCV transcriptionally upregulated the genes for phosphoenolpyruvate carboxykinase (PEPCK) and glucose 6-phosphatase (G6Pase), the rate-limiting enzymes for hepatic gluconeogenesis. In this way, HCV enhanced the cellular production of glucose 6-phosphate (G6P) and glucose. PEPCK and G6Pase gene expressions are controlled by the transcription factor forkhead box O1 (FoxO1). We observed that although neither the mRNA levels nor the protein levels of FoxO1 expression were affected by HCV, the level of phosphorylation of FoxO1 at Ser319 was markedly diminished in HCV-infected cells compared to the control cells, resulting in an increased nuclear accumulation of FoxO1, which is essential for sustaining its transcriptional activity. It was unlikely that the decreased level of FoxO1 phosphorylation was mediated through Akt inactivation, as we observed an increased phosphorylation of Akt at Ser473 in HCV-infected cells compared to control cells. By using specific inhibitors of c-Jun N-terminal kinase (JNK) and reactive oxygen species (ROS), we demonstrated that HCV infection induced JNK activation via increased mitochondrial ROS production, resulting in decreased FoxO1 phosphorylation, FoxO1 nuclear accumulation, and, eventually, increased glucose production. We also found that HCV NS5A mediated increased ROS production and JNK activation, which is directly linked with the FoxO1-dependent increased gluconeogenesis. Taken together, these observations suggest that HCV promotes hepatic gluconeogenesis through an NS5A-mediated, FoxO1-dependent pathway.

Hepatitis C virus (HCV) is a small, enveloped RNA virus that belongs to the genus *Hepacivirus* of the family *Flaviviridae*, and the molecular mechanisms underlying its viral replication are currently being unraveled (40). The HCV genome encodes a single polyprotein of about 3,000 amino acids, which is cleaved by host and viral proteases to generate at least 10 viral proteins, such as core, envelope 1 (E1), E2, p7, NS2, NS3, NS4A, NS4B, NS5A, and NS5B. HCV can be classified into seven genotypes, with each genotype further classified into a number of subtypes, such as HCV-1a and HCV-1b (18, 24, 59).

HCV infects more than 120 million people worldwide (57). Persistent HCV infection causes not only liver diseases (chronic hepatitis, liver cirrhosis, and hepatocellular carcinoma) but also extrahepatic manifestations, such as type 2 diabetes (2, 11, 20, 23). While it is known that liver cirrhosis impairs the glucose metabolism of the liver, there are some reports showing that HCV-infected patients over 40 years of age have an increased risk of type 2 diabetes compared with individuals without HCV infection (43). In addition, insulin receptor substrate 1 (IRS-1)/phosphatidylinositol 3-kinase (PI3-kinase) signaling was more impaired in HCV-infected patients than in non-HCV-infected controls (3). These studies imply that HCV infection may directly predispose the host toward type 2 diabetes. However, the precise mechanisms are poorly understood.

Hepatocytes play an important role in maintaining plasma glucose homeostasis by adjusting the balance between hepatic glucose production and utilization via the gluconeogenic and glycolytic pathways, respectively. It was proposed previously that increased hepatic glucose production is a major feature of type 2 diabetes (13). It is also known that hyperglycemia and the subsequent development of type 2 diabetes mellitus result, at least in part, from impaired insulin signaling together with elevated glucagon levels (5, 19). Hepatic glucose production and utilization, physiologically opposed cascades, are regulated, at least in part, at the transcriptional level of the glucose 6-phosphatase (G6Pase) and glucokinase (GK) genes, which catalyze the last and the first rate-limiting steps in gluconeogenesis and glycolysis, respectively. A number of studies have shown that fasting/feeding (or hormones) controls the transcription of these two enzymes in the opposite directions. G6Pase transcription is negatively regulated by insulin or feeding and is markedly increased in a fasting state (62). On the other hand, GK transcription is positively regulated by insulin or feeding and markedly decreased in a fasting state (33). It has also been reported that the gene expressions of gluconeogenic and glycolytic enzymes, such as G6Pase, GK, and phosphoenolpyruvate carboxykinase (PEPCK), another rate-limiting enzyme for hepatic gluconeogenesis, are regulated by certain

* Corresponding author. Mailing address: Division of Microbiology, Center for Infectious Disease, Kobe University Graduate School of Medicine, 7-5-1 Kusunoki-cho, Chuo-ku, Kobe 650-0017, Japan. Phone: 81-78-382-5500. Fax: 81-78-382-5519. E-mail: hotta@kobe-u.ac.jp.

[▽] Published ahead of print on 22 June 2011.

TABLE 1. Sequences and positions of primers used in this study

Gene (GenBank accession no.)	Primer	Positions	PCR product (bp)
GK (M69051)	5′-GCCTCCCAAAGCATCTACCTC-3′ 5′-GCTCCACTGCCCCTCCTCACC-3′	119–139 562–542	444
G6Pase (U01120)	5′-CCTGGGGCTGGCTCTCAACTC-3′ 5′-AATAGTAGTCCTCCTCAATCC-3′	889–909 1197–1177	309
PEPCK (BC023978)	5′-CCAGGCAGTGAGGGAGTTTCT-3′ 5′-ACTGTGTCTCTTTGCTCTTGG-3′	210–230 426–406	217
FoxO1 (NM_002915)	5′-GAGGGTTAGTGAGCAGGTTAC-3′ 5′-AGTCCTTATCTACAGCAGCAC-3′	2352–2372 2568–2548	217
HCV NS5A (JF343793)	5′-AGACGTATTGAGGTCCATGC-3′ 5′-CCGCAGCGACGGTGCTGATAG-3′	6899–6918 7011–7031	133
β-Glucuronidase (M15182)	5′-ATCAAAAACGCAGAAAATACG-3′ 5′-ACGCAGGTGGTATCAGTCTTG-3′	1747–1767 1984–1964	238
GAPDH (NM_002046)	5′-GCCATCAATGACCCCTTCATT-3′ 5′-TCTCGCTCCTGGAAGATGG-3′	196–216 326–344	149

transcription factors, including forkhead box O1 (FoxO1) (26, 50, 54), hepatic nuclear factor 4α (HNF-4α) (26), Krüppel-like factor 15 (KLF15) (64), and cyclic AMP (cAMP) response element binding protein (CREB) (52, 56). The deregulation of the otherwise balanced control of hepatic glucose homeostasis would potentially lead to hyperglycemia and, eventually, type 2 diabetes.

In this study, by using Huh-7.5 cells harboring HCV-1b RNA replicons, i.e., either a subgenomic RNA replicon (SGR) or a full-genomic RNA replicon (FGR) (37), and cells infected with HCV-2a (14, 37, 39), we investigated the possible effects of HCV on glucose metabolism. We report here that HCV promotes hepatic gluconeogenesis, resulting in increased cellular glucose production in hepatocytes via an NS5A-mediated, FoxO1-dependent pathway.

MATERIALS AND METHODS

Cells, HCV RNA replicons, and virus. The human hepatoma-derived cell line Huh-7.5 (7) was kindly provided by C. M. Rice (Rockefeller University, New York, NY). The SGR and FGR were prepared by using pFK5B/2884Gly (41) (a kind gift from R. Bartenschlager, University of Heidelberg, Heidelberg, Germany) and pON/C-5B (31) (a kind gift from N. Kato, Okayama University, Okayama, Japan), respectively. The SGR and FGR cells are of polyclonal origin to avoid clonal variation. Plasmid pFL-J6/JFH1, which encodes the entire viral genome of a chimeric strain of HCV-2a (J6/JFH1) (39), was kindly provided by C. M. Rice. The HCV RNA genome was transcribed *in vitro* from pFL-J6/JFH1 and transfected into Huh-7.5 cells to yield infectious HCV particles, as described previously (14). A cell culture-adapted P-47 strain (9, 14) was used throughout the experiments. Virus infection was performed at a multiplicity of infection (MOI) of 2.0. Virus infectivity was measured by indirect immunofluorescence analysis, as described below, and expressed as cell-infecting units/ml. In some experiments, SGR and FGR cells, as well as HCV-infected cells at 5 days after virus infection, were treated with 1,000 IU/ml of alpha interferon (IFN) (Sigma Chemical, St. Louis, MO) for 10 days to eliminate HCV replication.

Plasmid construction. Expression plasmids for core, p7, NS2, NS3, NS3/4A, NS4A, NS4B, NS5A, and NS5B were reported elsewhere previously (15, 32).

Real-time quantitative RT-PCR. Total cellular RNA was isolated by using RNAiso reagent (Takara, Kyoto, Japan), and cDNA was generated by using a QuantiTect reverse transcription (RT) system (Qiagen, Valencia, CA). Real-time quantitative PCR was performed by using SYBR Premix Ex *Taq* (Takara) with SYBR green chemistry on an ABI Prism 7000 system (Applied Biosystems, Foster City, CA), as reported previously (37). β-Glucuronidase and GAPDH (glyceraldehyde-3-phosphate dehydrogenase) were used as internal controls. The primers used are shown in Table 1.

G6P production assay. Huh-7.5 cells seeded into a 10-cm dish at a density of 1.0×10^6 cells/dish were infected with HCV or left uninfected. At different time points after infection, the cells were washed twice with 5% mannitol solution and covered with methanol (1 ml) containing 25 μM (each) four internal standards (3-aminopyrolidine, L-methionine sulfone, trimesate, and 2-morpholinoethanesulfonic acid) for enzyme inactivation. The mixtures of methanol and cells were collected and mixed with Milli-Q water and chloroform at ratios of 2:1:2. Both the medium and cell sample solutions were then centrifuged at 20,000 × *g* for 15 min, and the aqueous layers were collected for centrifugal filtration through a 5-kDa-cutoff filter at 9,000 × *g* for 2 h. The extracted metabolites were concentrated with a centrifugal concentrator and stored at −80°C until analysis. Glucose 6-phosphate (G6P) concentrations were measured by capillary electrophoresis time-of-flight mass spectrometry (CE-TOFMS), and the results were normalized to the cell number as described previously (60, 61).

Glucose production assay. Culture medium was replaced with glucose production buffer consisting of glucose-free Dulbecco's modified Eagle's medium (DMEM) (Sigma Chemical), without phenol red, supplemented with a gluconeogenic substrate (2 mM sodium pyruvate and 20 mM sodium lactate). After 24 h of incubation, the medium was collected, and the total glucose concentration was measured by using a commercial kit (Glucose CII Test Wako; Wako Pure Chemical Industries, Osaka, Japan) and normalized to the cellular protein content. As the baseline of glucose production, glucose-free DMEM with neither sodium pyruvate nor sodium lactate was used. Glucose production via gluconeogenesis equals the total glucose production minus the baseline glucose production.

Luciferase reporter assay. The PEPCK gene promoter (position −1263/+225) and a deletion mutant (position −998/+225) were inserted into the pGL3 luciferase reporter plasmid (Promega, Madison, WI). The constructs were designated rPEPCK-P5(−1263)-pGL3basic and rPEPCK-P4(−998)-pGL3basic. pRL-CMV-Renilla (Promega), which expresses *Renilla* luciferase, was used as an internal control. Huh-7.5 cells prepared in a 12-well tissue culture plate at a density of 1.0×10^5 cells/well were transiently transfected with pRL-CMV-Renilla and rPEPCK-P5(−1263)-pGL3basic or rPEPCK-P4(−998)-pGL3basic in the presence of pEF1/NS4A, pEF1/NS5A, or a control vector (32). After 48 h, a luciferase assay was performed by using the Dual-Luciferase reporter assay system (Promega). Firefly and *Renilla* luciferase activities were measured with a Lumat LB 9501 luminometer (Berthold, Bad Wildbad, Germany). Firefly luciferase activity was normalized to *Renilla* luciferase activity for each sample.

Detection of mitochondrial ROS. Mitochondrial reactive oxygen species (ROS) production was analyzed as described previously (14). Briefly, cells seeded onto glass coverslips in a 24-well plate were incubated with 5 μM MitoSOX red (Molecular Probes, Eugene, OR) at 37°C for 10 min and then fixed with 3.7% paraformaldehyde and observed under a confocal laser scanning microscope (Carl Zeiss, Oberkochen, Germany). When needed, the fixed cells

were subjected to indirect immunofluorescence analysis to confirm HCV infection or NS5A expression, as described below.

Indirect immunofluorescence. Huh-7.5 cells seeded onto glass coverslips in a 24-well plate were infected with HCV or transfected with an NS5A expression plasmid. At 5 days postinfection (dpi) or 3 days posttransfection, the cells were fixed with 3.7% paraformaldehyde in phosphate-buffered saline (PBS) for 15 min at room temperature and permeabilized with 0.1% Triton X-100 in PBS for 15 min at room temperature. Mock-infected or empty-vector-transfected cells were similarly treated as controls for comparisons. After being washed with PBS twice, cells were consecutively stained with primary and secondary antibodies. The primary antibodies used were anti-FoxO1 rabbit monoclonal antibody (Cell Signaling Technology, Danvers, MA), anti-NS5A mouse monoclonal antibody (Chemicon International, Temecula, CA), and serum from an HCV-infected patient. Secondary antibodies used were Alexa Fluor 488-conjugated goat anti-rabbit immunoglobulin G (IgG), Alexa Fluor 594-conjugated goat anti-mouse IgG or anti-human IgG (Molecular Probes), and fluorescein isothiocyanate (FITC)-conjugated goat anti-mouse IgG or anti-human IgG (MBL, Nagoya, Japan). The stained cells were observed under a confocal laser scanning microscope (Carl Zeiss).

Cell fractionation and immunoblotting. Nuclear and cytoplasmic extracts from cells were prepared by using an NE-PER nuclear and cytoplasmic extraction reagent kit (Pierce Chemical, Rockford, IL). For immunoblotting, cells were lysed with SDS sample buffer, and equal amounts of protein were subjected to SDS-polyacrylamide gel electrophoresis and transferred onto a polyvinylidene difluoride membrane (Millipore, Bedford, MA), which was then incubated with the respective primary antibodies. The primary antibodies used were mouse monoclonal antibodies against HCV core (clone 2H9; a kind gift from T. Wakita, Department of Virology II, National Institute of Infectious Diseases, Tokyo, Japan), NS3, NS4A, NS5A, GAPDH (Chemicon), FoxO1 (Sigma Chemical), phospho-Akt (Ser473) (Cell Signaling Technology), and c-Myc (9E10; Santa Cruz Biotechnology, Santa Cruz, CA); rabbit polyclonal antibodies against phospho-FoxO1 (Ser139), Oct-1 (Santa Cruz Biotechnology), c-Jun N-terminal kinase (JNK), phospho-JNK (Thr183/Tyr185), c-Jun, phospho-c-Jun (Ser63), and Akt (Cell Signaling Technology); and goat polyclonal antibody against HSP60 (Santa Cruz Biotechnology). Horseradish peroxidase-conjugated goat anti-mouse IgG, goat anti-rabbit IgG (Molecular Probes), and donkey anti-goat IgG (Santa Cruz Biotechnology) were used to visualize the respective proteins by means of an enhanced chemiluminescence detection system (ECL; GE Healthcare, Buckinghamshire, United Kingdom).

Statistical analysis. Results were expressed as means ± standard errors of the means (SEM). Statistical significance was evaluated by analysis of variance (ANOVA) and was defined as a P value of <0.05.

RESULTS

HCV upregulates gene expression of PEPCK and G6Pase and downregulates gene expression of GK. We first examined the expression levels of the genes for the rate-limiting enzymes in hepatic gluconeogenesis, PEPCK and G6Pase, and of those for GK, which catalyzes the first step of glycolysis, by means of real-time quantitative RT-PCR analysis. We observed that the PEPCK and G6Pase genes were transcriptionally activated in SGR- and FGR-harboring cells (Fig. 1A and B, left). Similarly, the PEPCK and G6Pase genes were upregulated in HCV-infected cells in a time-dependent manner, starting from 3 or 5 days postinfection (dpi) up to 14 dpi (Fig. 1A and B, middle). On the other hand, the GK gene was transcriptionally downregulated in SGR- and FGR-harboring cells and HCV-infected cells in a time-dependent manner (Fig. 1C). It is noteworthy that the gene expressions of six glycolytic enzymes (not including GK) were observed to be upregulated in HCV-infected cells at 1 dpi (16).

When IFN treatment eliminated HCV from the cells, the observed upregulation of PEPCK and G6Pase gene expressions as well as the downregulation of GK gene expression in SGR- and FGR-harboring cells and HCV-infected cells were cancelled (Fig. 1A, B, and C, left and right). Thus, our results suggest that there was a trend toward an increase in gluconeogenesis in SGR- and FGR-harboring cells and HCV-infected cells. In subsequent studies we further examined whether or not HCV replication was correlated with gluconeogenesis.

HCV promotes cellular production of glucose and G6P. We then examined the effect of HCV on cellular glucose production. The results showed that SGR- and FGR-harboring cells and HCV-infected cells produced greater amounts of glucose than did the control cells (Fig. 2A, top and middle). IFN treatment cancelled the enhanced glucose production in SGR- and FGR-harboring cells and in HCV-infected cells (Fig. 2A, top and bottom). We also investigated the production of G6P, which is an important precursor molecule that is converted to glucose in the gluconeogenesis pathway, by means of metabolome analysis. As shown in Fig. 2B, a significantly higher level of G6P was accumulated in HCV-infected cells than in control cells. Taken together, these results indicate that HCV indeed promotes hepatic gluconeogenesis to cause hyperglycemia. In the following analyses, we examined the possible mechanisms of HCV-induced increased gluconeogenesis.

HCV suppresses FoxO1 phosphorylation at Ser319, leading to the nuclear accumulation of FoxO1. It was demonstrated previously that FoxO1 in hepatocytes enhances gluconeogenesis through the transcriptional activation of various genes, including G6Pase and PEPCK (25). To investigate the possible effects of FoxO1 on HCV-induced gluconeogenesis, we examined the gene expression levels of FoxO1 by real-time quantitative RT-PCR analysis. As shown in Fig. 3A, there was neither an upregulation nor a downregulation of FoxO1 gene expression in SGR- or FGR-harboring cells or HCV-infected cells. The FoxO1 transcription factor is controlled by various post-translational modifications, which include phosphorylation, ubiquitylation, and acetylation. The phosphorylated form of FoxO1 is exported from the nucleus and thereby loses its transcriptional function (30). We therefore examined the phosphorylation status of FoxO1 at Ser319, which is critical for FoxO1 nuclear exclusion (72). The results showed that FoxO1 phosphorylation at Ser319 was markedly suppressed in HCV-infected cells from 4 dpi up to 8 dpi, compared to that in the HCV-negative control cells (Fig. 3B, first panel), in a time-dependent manner that was roughly the inverse of the pattern observed for PEPCK and G6Pase mRNA upregulations (Fig. 1A and B) and glucose production (Fig. 2A), while the total protein expression levels of FoxO1 were unchanged (Fig. 3B, second panel). Regarding this connection, Banerjee et al. reported previously that FoxO1 phosphorylation at Ser256 was also inhibited in HCV-infected cells (4). Since FoxO1 is known to be phosphorylated by Akt so as to be exported from the nucleus and transcriptionally inactivated (38), we examined whether Akt function was suppressed through its impaired phosphorylation in HCV-infected cells. The result obtained revealed that this was not the case: Akt phosphorylation was enhanced in HCV-infected cells from 4 dpi up to 6 dpi compared with the control cells (Fig. 3B, third panel), while the total protein expression levels of Akt were comparable (Fig. 3B, fourth panel). This result is consistent with a recent observation by Burdette et al. (10) showing that the Akt phosphorylation level was elevated in HCV-infected cells. These data suggest that the observed decrease in FoxO1 phosphorylation

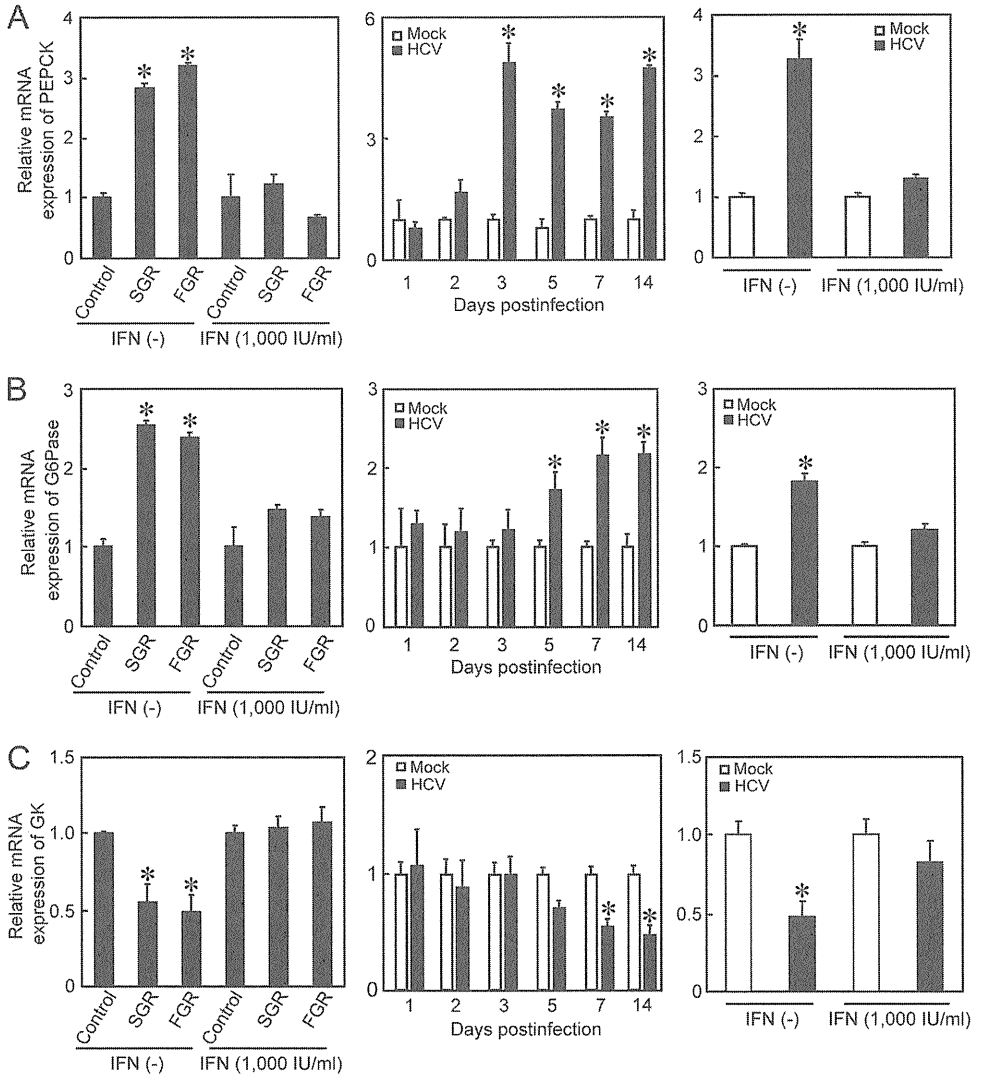

FIG. 1. HCV upregulates gene expressions of PEPCK and G6Pase and downregulates gene expression of GK. Quantitative RT-PCR analysis was performed to quantify PEPCK (A), G6Pase (B), and GK (C) mRNA expression levels in SGR- and FGR-harboring cells and HCV-infected cells (MOI = 2), and the results were normalized to β-glucuronidase mRNA expression levels. In parallel, SGR- and FGR-harboring cells and HCV-infected cells (at 5 dpi) were treated with IFN (1,000 IU/ml) for 10 days to eliminate HCV replication before being subjected to quantitative RT-PCR. Data represent means ± SEM of data from three independent experiments, and the values for the control cells were arbitrarily expressed as 1.0. *, $P < 0.01$ compared with the control.

in HCV-infected cells is caused by a mechanism independent of Akt.

Next, we tested whether HCV indeed promoted FoxO1 nuclear accumulation. The majority of FoxO1 was accumulated in the nuclear fraction in HCV-infected cells (Fig. 3C, second panel, lanes 2 and 4), whereas in control cells FoxO1 was distributed in both the nuclear and cytoplasmic fractions (lanes 1 and 3). Taken together, these results suggest that HCV suppressed FoxO1 phosphorylation, leading to the nuclear accumulation of FoxO1.

HCV-induced JNK activation is involved in the suppression of FoxO1 phosphorylation. Recent studies demonstrated that a signaling pathway that involves the stress-sensitive serine/threonine kinase JNK regulates FoxO at multiple levels (36, 66). We therefore investigated whether HCV induced JNK activation in Huh-7.5 cells. As shown in Fig. 4A, the amount of phosphorylated (activated) JNK markedly increased in HCV-infected cells in a time-dependent manner, similar to that observed for the suppression of FoxO1 phosphorylation, while the total expression levels of JNK were unchanged. As a result, c-Jun, a key substrate for JNK, was phosphorylated (activated) in HCV-infected cells but not in the mock-infected control cells. It should also be noted that the total expression levels of c-Jun in HCV-infected cells were significantly higher than those in the mock-infected control cells, suggesting that c-Jun activation through its phosphorylation stabilizes c-Jun protein expression in HCV-infected cells, as was proposed previously by Zhang et al (71).

We next sought to determine whether JNK activation was involved in the HCV-induced suppression of FoxO1 phosphorylation. HCV-infected cells at 5 days after virus infection were treated with the specific JNK inhibitor SP600125 (20 μM) (6)

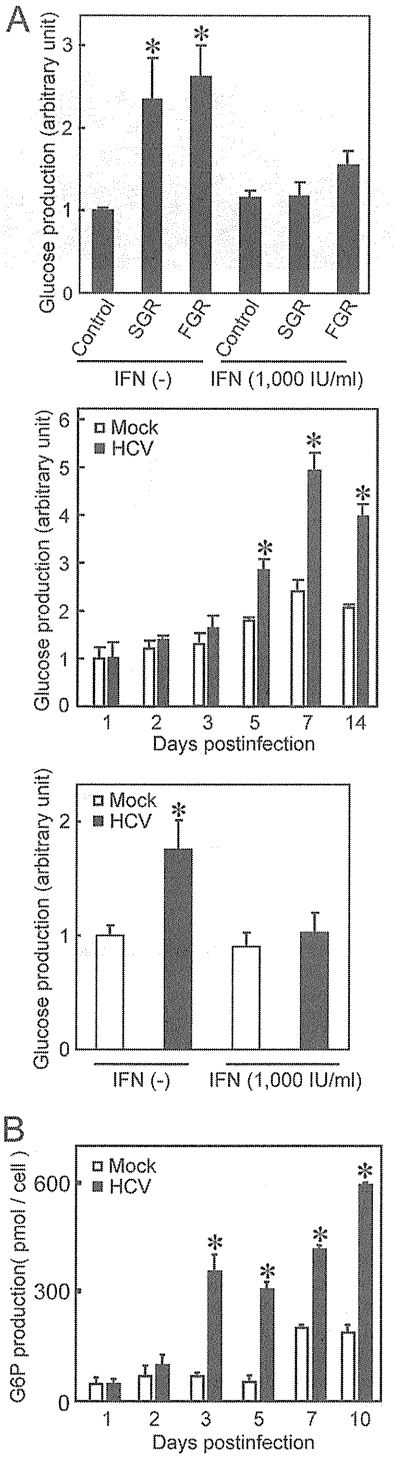

FIG. 2. HCV promotes the production of glucose and G6P. (A) Extracellular glucose production was measured in SGR- and FGR-harboring cells and HCV-infected cells (MOI = 2) and normalized to total cellular protein expression levels. In parallel, SGR- and FGR-harboring cells and HCV-infected cells (at 5 dpi) were treated with IFN (1,000 IU/ml) for 10 days to eliminate HCV replication before being subjected to glucose production analysis. Data represent means ± SEM of data from three independent experiments, and the value for the control cells was arbitrarily expressed as 1.0. *, $P < 0.01$ compared with the control. (B) Cellular G6Pase production was measured in HCV-infected cells (MOI = 2), and the results were normalized to cell numbers. Data represent means ± SEM of data from three independent experiments. *, $P < 0.01$ compared with the control.

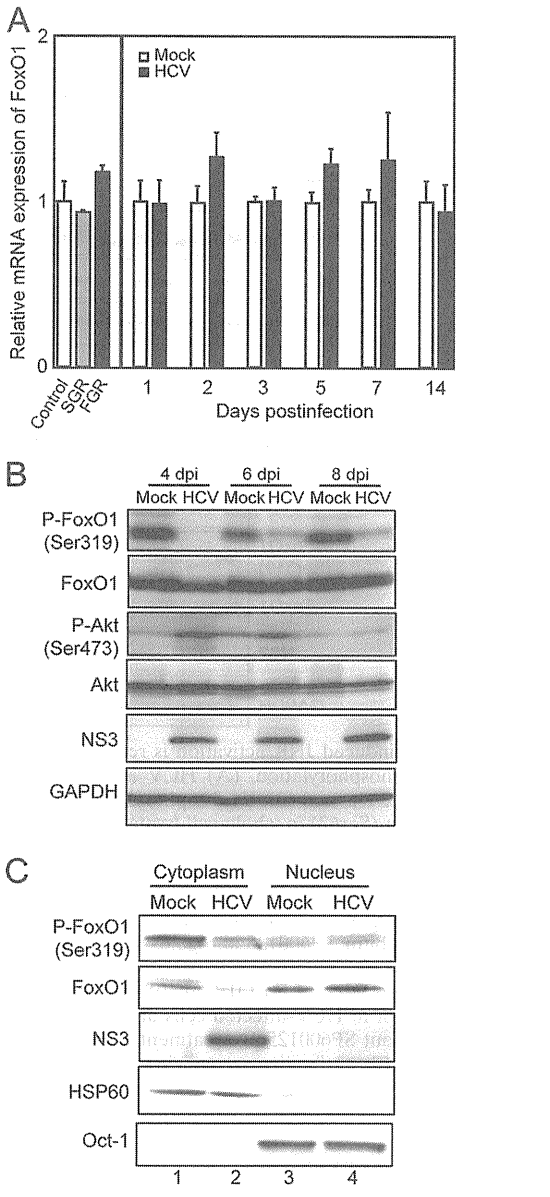

FIG. 3. HCV suppresses FoxO1 phosphorylation, leading to nuclear accumulation of FoxO1. (A) Quantitative RT-PCR analysis was performed to determine FoxO1 mRNA expression levels in SGR- and FGR-harboring cells and HCV-infected cells (MOI = 2), and expression levels were normalized to β-glucuronidase mRNA expression levels. (B) The expression levels of FoxO1, phospho-FoxO1 (Ser319) (P-FoxO1), Akt, and phospho-Akt (Ser473) were analyzed by immunoblotting of HCV-infected cells and mock-infected control cells. Blots were reprobed with antibodies recognizing NS3 and GAPDH. The amounts of GAPDH were measured as an internal control to verify equal amounts of sample loading. (C) Cytoplasmic and nuclear fractions were prepared from HCV-infected cells and mock-infected control cells at 4 dpi and were analyzed by immunoblotting using antibodies against FoxO1, phospho-FoxO1 (Ser319), NS3, Hsp60, and Oct-1. The amounts of Hsp60 and Oct-1 were measured to verify that they were equal to the amounts of cytoplasmic and nuclear fractions, respectively.

for 24 h. The catalytic JNK activity was assayed by monitoring the phosphorylation of c-Jun. As shown in Fig. 4B, SP600125 clearly prevented the phosphorylation of c-Jun and concomitantly recovered the suppression of FoxO1 phosphorylation in

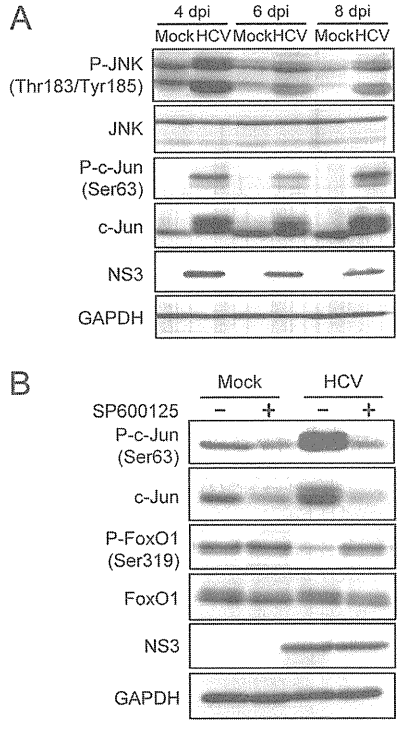

FIG. 4. HCV-induced JNK activation is required for the suppression of FoxO1 phosphorylation. (A) HCV activates the JNK/c-Jun signaling pathway. The activation (phosphorylation) of JNK (Thr183/Tyr185) and c-Jun (Ser63) in whole-cell lysates of HCV-infected cells and mock-infected control cells was analyzed by immunoblotting. Blots were reprobed with antibodies recognizing total JNK and c-Jun, NS3, and GAPDH. The amounts of GAPDH were measured as an internal control to verify equal amounts of sample loading. (B) Pretreatment with the JNK inhibitor SP600125 abrogates HCV-induced c-Jun activation and FoxO1 phosphorylation suppression. The phosphorylation of c-Jun (Ser63) and that of FoxO1 (Ser319) were analyzed by immunoblotting at 6 dpi in HCV-infected cells and mock-infected control cells with or without SP600125 pretreatment (20 μM for 24 h). Blots were reprobed with antibodies recognizing total c-Jun and FoxO1, NS3, and GAPDH. The amounts of GAPDH were measured as an internal control to verify equal amounts of sample loading.

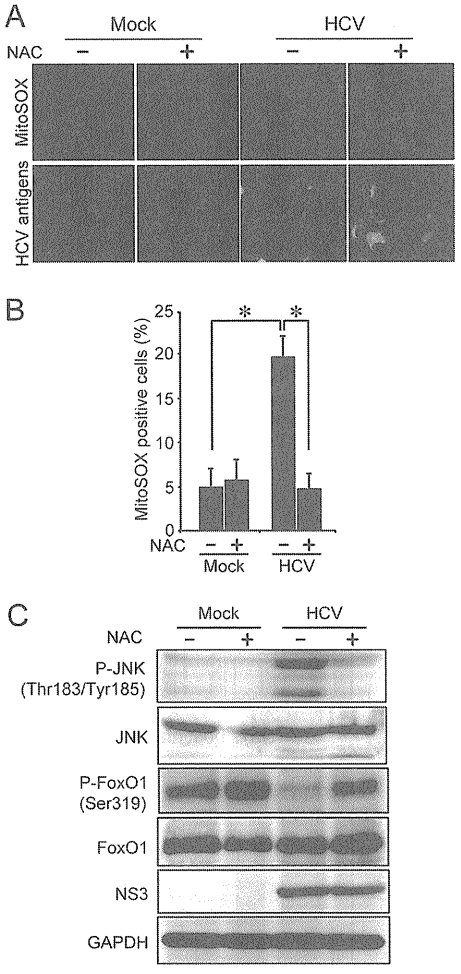

FIG. 5. HCV-induced production of mitochondrial ROS suppresses FoxO1 phosphorylation through activation of JNK. (A) Pretreatment with NAC abrogates the HCV-induced increased production of mitochondrial ROS. HCV-infected cells and mock-infected controls were pretreated with 5 mM NAC for 2 h at 6 dpi. The cells were then incubated with MitoSOX (top) and then stained for HCV antigens by using serum from an HCV-infected patient, followed by FITC-conjugated goat anti-human IgG (bottom). (B) Quantification of MitoSOX-stained cells. The percentages of cells stained with MitoSOX were determined for HCV-infected cells and mock-infected controls with or without NAC pretreatment. Data represent means ± SEM of data from two independent experiments. *, $P < 0.01$. (C) NAC pretreatment abrogates HCV-induced JNK activation and FoxO1 phosphorylation suppression. The phosphorylation of JNK (Thr183/Tyr185) and that of FoxO1 (Ser319) were analyzed by immunoblotting at 6 dpi in HCV-infected cells and mock-infected controls with or without NAC pretreatment (5 mM for 2 h). The blots were reprobed with antibodies recognizing total JNK and FoxO1, NS3, and GAPDH. The amounts of GAPDH were measured as an internal control to verify equal amounts of sample loading.

HCV-infected cells. These results suggest that HCV activates the JNK/c-Jun signaling pathway, which induces the nuclear accumulation of FoxO1 by reducing its phosphorylation status.

HCV-induced mitochondrial ROS production is involved in FoxO1 phosphorylation suppression, FoxO1 nuclear accumulation, and increased glucose production through JNK activation. We previously reported that HCV infection increases mitochondrial ROS production (14). JNK is known to be activated by ROS (35). We therefore sought to determine whether the HCV-induced increase in ROS production is an event occurring upstream of JNK activation by HCV. The pretreatment of HCV-infected cells (at 6 dpi) with 5 mM *N*-acetyl cysteine (NAC) (a general antioxidant) for 2 h significantly reduced the HCV-induced increase in ROS levels (Fig. 5A and B), as revealed by using MitoSOX, a fluorescent probe specific for superoxide that selectively accumulates in the mitochondrial compartment. As shown in Fig. 5C, NAC clearly prevented the phosphorylation of JNK and concomitantly recovered the suppression of FoxO1 phosphorylation in HCV-infected cells. These results suggest that HCV-induced ROS production is involved in JNK activation, which results in the inhibition of FoxO1 phosphorylation.

We next investigated the effects of JNK activation and ROS production on the subcellular localization of FoxO1 in HCV-infected cells by indirect immunofluorescence staining. As shown in Fig. 6A and B, FoxO1 was localized predominantly in the cytoplasm of mock-infected control cells. On the other